Journal of Medicinal Chemistry

Article

pubs.acs.org/jmc

Discovery of (*S*)-1-(1-(Imidazo[1,2-*a*]pyridin-6-yl)ethyl)-6-(1-methyl-1*H*-pyrazol-4-yl)-1*H*-[1,2,3]triazolo[4,5-*b*]pyrazine (Volitinib) as a Highly Potent and Selective Mesenchymal−Epithelial Transition Factor (c-Met) Inhibitor in Clinical Development for Treatment of Cancer

Hong Jia,[†] Guangxiu Dai,[†] Jianyang Weng, Zhulin Zhang, Qing Wang, Feng Zhou, Longxian Jiao, Yumin Cui, Yongxin Ren, Shiming Fan, Jinghong Zhou, Weiguo Qing, Yi Gu, Jian Wang, Yang Sai, and Weiguo Su*,[†]

Hutchison MediPharma Limited, Building 4, 720 Cai Lun Road, Zhangjiang Hi-Tech Park, 201203, Shanghai, China

Supporting Information

ABSTRACT: HGF/c-Met signaling has been implicated in human cancers. Herein we describe the invention of a series of novel triazolopyrazine c-Met inhibitors. The structure−activity relationship of these compounds was investigated, leading to the identification of compound **28**, which demonstrated favorable pharmacokinetic properties in mice and good antitumor activities in the human glioma xenograft model in athymic nude mice.

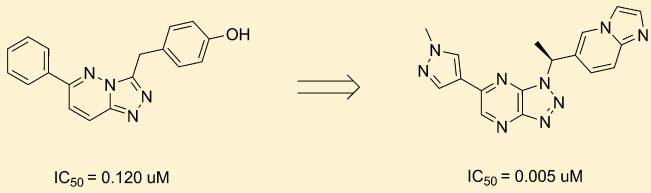

INTRODUCTION

Mesenchymal−epithelial transition factor (c-Met), a member of a structurally distinct family of receptor tyrosine kinases (RTK), is a proto-oncogene encoding the high affinity receptor for hepatocyte growth factor (HGF).[1,2] The Met protein is expressed mainly by epithelial cells, and its endogenous ligand (HGF) is restricted to cells of mesenchymal origin.[3,4] HGF/c-Met signaling mediates a diverse array of biological activities, including proliferation, survival, motality, migration, branching morphogenesis, wound healing and angiogenesis. These activities are not only essential during embryogenesis and tissue repair, but they also contribute to cancer progression by enabling tumor cell proliferation, survival, invasion, metastasis, and angiogenesis. c-Met-dependent cellular proliferation can occur in response to activating mutations, gene amplification, or via overexpression.[5,6]

As a result of its central role in tumor cell biology, c-Met has been targeted by several drug discovery programs. These have enjoyed limited success. In particular, while drug candidates acting on c-Met have entered clinical trials, so far none of them has been approved. c-Met ATP-competitive inhibitors of the first generation have broad kinase activities, usually targeting other kinases besides c-Met. For example, XL880 is an inhibitor of c-Met and vascular endothelial growth factor receptor 2 (VEGFR2).[7] BMS-777607 is a c-Met inhibitor with additional activities against related kinases such as AXL receptor tyrosine kinase (Axl) and Recepteur d'Origine Nantais Kinase (Ron), respectively.[8] c-Met ATP-competitive inhibitors of the second generation are relatively selective. Chemically, these second generation c-Met inhibitors in clinical development all share a relatively conserved structure. In particular, the compounds all contain a quinoline moiety, which appears to be critical for selective binding to the enzyme. For example, PF-04217903 showed potent and selective c-Met inhibition.[9] JNJ-38877605, another selective c-Met inhibitor, was terminated in phase I clinical study due to an increase in serum creatinine levels, suggestive of renal toxicity and minimal pharmacodynamic (PD) activity.[10,11] Similarly, SGX523 was discontinued in clinical development because of unexpected renal failure. This toxicity has been hypothesized to arise as a result of insoluble metabolites generated by aldehyde oxidase (AO) precipitating in the kidney and causing mechanical damage[12,13] (Figure 1).

Therefore, while the conserved structure of the second generation c-Met inhibitors delivers selectivity, it also has toxicity liabilities. Here, we wish to report the discovery of a novel ATP-competitive kinase inhibitor which is structurally differentiated from the known inhibitors (in particular lacking the hitherto ubiquitous quinoline group) but surprisingly maintains potent activity and exquisite kinase selectivity for c-Met. It is hoped that this compound may avoid the reported toxicity issues seen in the earlier c-Met therapies, particularly since the compound is fairly stable to AO metabolism, and both the parent compound and its AO metabolite are relatively soluble in aqueous medium. This should ensure that any products by AO metabolism should remain dissolved in the urine, minimizing any risk of the nephropathy seen in earlier therapeutic candidates.

Received: March 31, 2014
Published: August 22, 2014

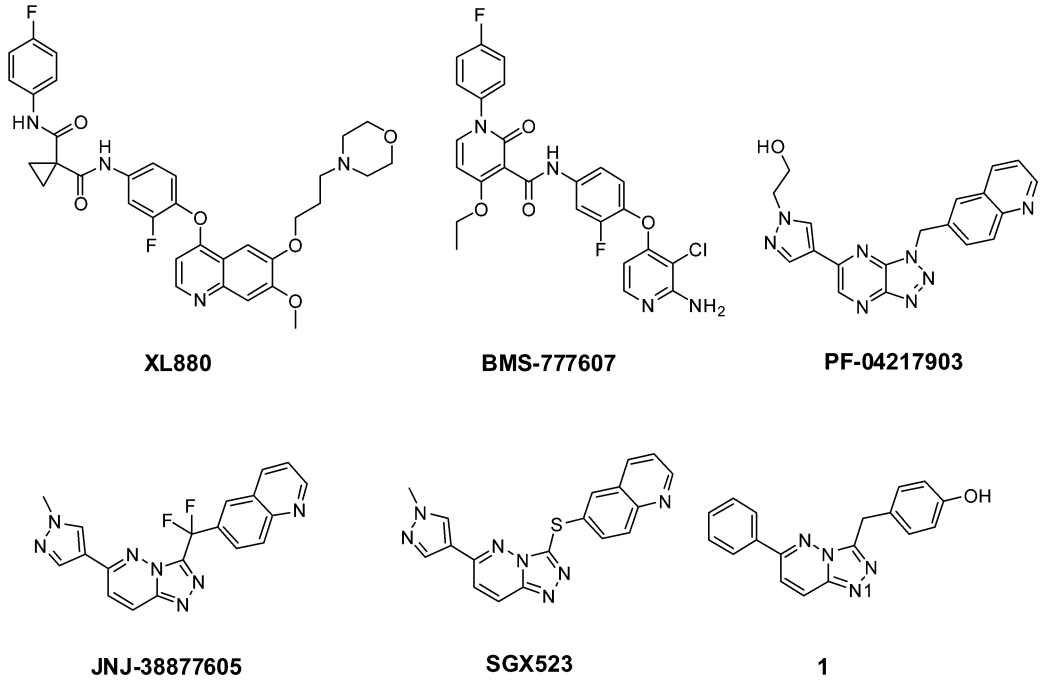

Figure 1. Reference compounds.

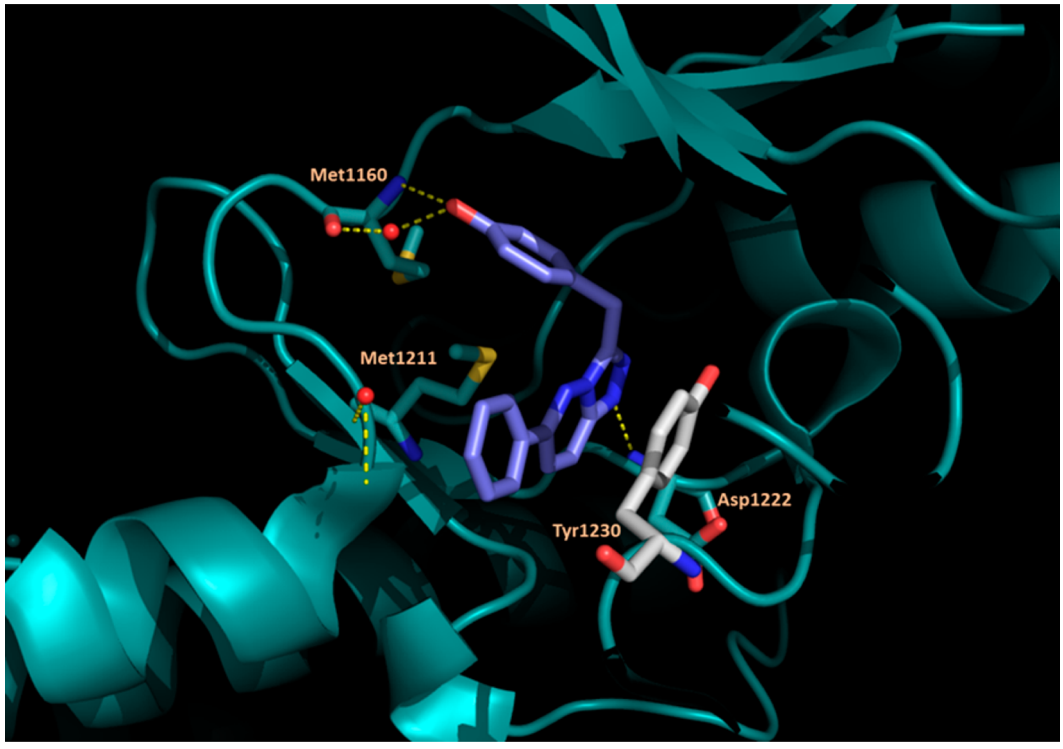

Figure 2. Co-crystal structure of **1** with c-Met.[14] Amgen reported the co-crystal structure of **1** and c-Met. PDB code: 3CCN.

RESULTS AND DISCUSSION

Amgen previously reported **1** as a c-Met inhibitor with an IC_{50} of 0.120 μM in an enzyme assay. Its co-crystal structure revealed a unique binding mode (Figure 2): (1) a bent "U-shaped" conformation with the inhibitor wrapped around Met1211; (2) a hydrogen bond between the backbone NH of Met1160 and the oxygen of the phenol, the hinge binder; (3) a hydrogen-bonding interaction between N1 of the inhibitor and the backbone NH of Asp1222; and (4) a $\pi-\pi$ stacking interaction between the triazolopyridazine core and Tyr1230.[14] Although no other binding information was reported with selective inhibitors except **1**, 6 years ago, considering the high similarity of their structures and corresponding enzyme selectivity, it is reasonable to assume that c-Met ATP-competitive inhibitors of the second generation also adopt a U-shaped conformation and are bound to the activation loop of c-Met kinase the same way, which was confirmed by several subsequent publications.[10,15,16]

dx.doi.org/10.1021/jm500510f | J. Med. Chem. 2014, 57, 7577−7589

To better understand the influence of the core structure on the U-shaped binding mode between the inhibitor and the kinase, we first investigated structure types having an N possible for binding with Asp1222 of the c-Met enzyme and a quinoline moiety to retain the hydrogen bond with the backbone NH of Met1160, but with variable central heterocylic groups.

An enzymatic assay to measure the ability of a compound to inhibit the c-Met kinase and a cellular assay to assess the inhibition effect on phosphorylation of c-Met kinase were used as the primary screening assays. As shown in Table 1, both compounds **2** and **5** demonstrated high biochemical potency toward c-Met with an IC_{50} of 0.005 and 0.012 μM, respectively. However, compound **5** exhibited only moderate inhibitory activity on phosphorylation in the cellular assay. By removing N2 in compounds **2** and **5**, compounds **3** and **6** displayed lower c-Met kinase activities. When the N7 of compound **2** was replaced by a C7, the corresponding analog **4** was not active against c-Met with IC_{50} > 1 μM. Moving N4 of compound **2** to N5, the resulting compound **7** also led to the loss of c-Met activity. Compound **8** with a bridge nitrogen showed similar potency in both enzymatic and celluar assays as compound **5**. Clearly the electronic property of the cores has a great effect on the π-stacking interaction with Tyr1230. The most potent core, [1,2,3]triazolo[4,5-*b*]pyrazine in **2**, was selected for further structure–activity relationship (SAR) exploration.

Table 1. SAR of the Core

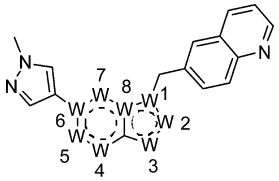

compound	core	IC_{50} [a] (μM)		compound	core	IC_{50} [a] (μM)	
		enzyme	p-Met			enzyme	p-Met
2		0.005	0.006	**5**		0.012	0.093
3		0.096	0.120	**6**		0.460	--[b]
4		>1	--[b]	**7**		>1	--[b]
8		0.021	0.069				

[a] IC_{50S} are based on single runs of experiments. [b] The -- indicates not tested.

To introduce further structural differentiation from c-Met inhibitors with known toxicity liabilities, we now began to identify a chemical moiety to replace the quinoline hinge motif. Several heteroaryls were investigated as new hinge pieces. As shown in Table 2, these heteroaryls demonstrated variable c-Met inhibition activities compared to quinoline in **2**. 2-Substituted pyrrolo[2,3-*b*]pyridine **9** reduced the potency significantly, and 3-substituted pyrrolo[2,3-*b*]pyridine **10** was 40-fold more potent with an IC_{50} of 0.005 μM than compound **9** in the enzymatic assay. Pyrazolo[3,4-*b*]pyridine **11** with one more N atom was also very potent against c-Met in both enzymatic and cellular assays. 3-Substituted thieno[2,3-*b*]-pyridine **12** and 2-substituted thieno[2,3-*b*]pyridine **13** exhibited much lower potency. The regioisomer thieno[3,2-*c*]pyridine **14** was 17-fold more potent (IC_{50} is 0.011 μM in the enzymatic assay) than **13**. Thieno[3,2-*c*]pyrazole **15** with a pyrazole replacing the pyridine of **13** greatly improved the potency more than 30-fold with an IC_{50} of 0.006 μM in enzyme and 0.019 μM in cell. This proved the position of N on the hinge piece is crucial for the binding with the backbone NH of Met 1160, and the NH of **10**-**11** and **15** may also contribute to the binding as a potential hydrogen donor. Imidazo[1,2-

Table 2. SAR of the Hinge Pieces

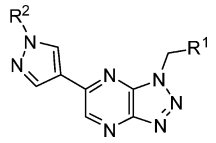

compound	R^1	R^2	IC_{50} [a] (μM)			MLM [b] parent drug remaining (%)
			c-Met enzyme	p-Met	proliferation	
2		Me	0.005	0.006	--[c]	--[c]
9		CH_2CH_2OH	0.227	--[c]	--[c]	--[c]
10		CH_2CH_2OH	0.005	0.010	0.025	82.6
11		Me	0.009	0.006	0.066	102.1
12		Me	0.378	--[c]	--[c]	--[c]
13		Me	0.194	--[c]	--[c]	--[c]
14		Me	0.011	0.061	0.177	23.5
15		Me	0.006	0.019	0.178	19.4
16		Me	0.006	0.011	0.073	70.8
17		Me	0.13	--[c]	--[c]	--[c]
18		Me	0.026	0.077	0.425	--[c]
19		Me	0.024	0.063	0.443	--[c]
20		Me	0.019	0.020	0.183	36.7
21		Me	0.142	--[c]	--[c]	--[c]
22		Me	0.359	--[c]	--[c]	--[c]

[a] IC_{50S} are based on single runs of experiments. [b] Mouse liver microsome stability. [c] The -- indicates not tested.

dx.doi.org/10.1021/jm500510f | J. Med. Chem. 2014, 57, 7577–7589

a]pyridine **16** was highly potent (IC_{50} is 0.006 μM in enzyme and 0.011 μM in phosphorylation), but imidazo[1,2-*a*]pyrazine **17**, [1,2,4]triazolo[1,5-*a*]pyridine **18**, and imidazo[1,2-*b*]-pyridazine **19** with one more N all had decreased potencies in both enzymatic and cellular assays. Similarly, pyrazolo[1,5-*a*]pyridine analogue **20** was much more potent than the corresponding *aza* analogues pyrazolo[1,5-*a*]pyrimidine **21** and [1,2,4]triazolo[1,5-*a*]pyridine **22** indicating a strong electronic effect on the binding of the hinge piece with the backbone NH of Asp1222.

In summary, quinolone as a hinge binder could be replaced by other heteroaryl moieties that retained potency against c-Met. Although many of the compounds in Table 2 demonstrated good potencies in both enzymatic and cellular assays with $IC_{50} \leq 0.1$ μM, HGF-induced proliferation assay in NCI-H441 cell line, a functional assay which has a better correlation with the in vivo target inhibition, suggested that the hinge binders in compounds **10**, **11**, **14**−**16**, and **20** are interesting. Further profiling study showed that **14** and **15** had poor stabilities in mouse liver microsomes with only 23.5% and 19.4% remaining after incubation for 30 min.

To further define the SAR and improve the potency of **11**, **16**, and **20** series, a variety of substitutes at the 6-position of triazolopyrazine core were explored. As shown in Table 3, except **27B**, all compounds showed very potent inhibition in both enzymatic and cellular assays. Among them, **23C**, **24A**, **24C**, and **26B** demonstrated most potent proliferation inhibition in NCI-H441 cell line, but **26B** was unstable in mouse liver microsomes with only 23.4% remaining after incubation for 30 min.

Compound **10**, **11**, **16**, **23C**, **24A**, and **24C** were subsequently evaluated in HGF-mediated c-Met phosphorylation in NCI-H441 in vivo in the tumor bearing mice. Figure 3 illustrates that these compounds only showed weak to moderate inhibition at 6 h after a single oral dose of 3 mg/kg.

The selected compounds **11**, **16**, and **23C** were further evaluated in the preliminary pharmacokinetic studies in mice. Injection dosing with compound **11** caused sudden death of mice at the levels of 2.5 and 1.25 mg/kg. The reason for animal death was not clear. The compound was therefore deprioritized. As Table 4 shows, compound **16** was rapidly cleared in vivo. The short $T_{1/2}$ might explain its weak inhibition at 6 h in the in vivo HGF-induced c-Met phosphorylation study. Compound **23C** had desirable pharmacokinetical properties with high exposure and bioavailability, but the moderate activity in in vivo target inhibition assay indicates an IC_{50} of 0.066 μM in the proliferation assay was not good enough to provide robust activity in the NCI-H441 assay.

Since the methylene attached to an aromatic ring is easily metabolized by oxidation, the introduction of a group to block the possible metabolism may help reduce the clearance.[17] The co-crystal of **1** with c-Met kinase revealed that methylene was adjacent to a hydrophobic pocket with Leu-1157, Lys-1110, and Val-1092 residues. A small hydrophobic group on the methylene group may go into the pocket to form hydrophobic interaction with the kinase. We therefore investigated small modifications of the bridging methylene group. As shown in Table 5, after introduction of a methyl, enantiomerically pure compounds **28**−**31** demonstrated good inhibition of c-Met activity. Compared with unbranched compounds **16** and **23C**, compounds **28** and **30**, respectively, had equal activities against c-Met kinase and slightly better potency in cellular assays. More significantly, their abilities to inhibit HGF-induced proliferation were improved. Especially compound **28** inhibited proliferation 12-fold more potently than compound **16**. Compounds **28** and **30** with an (*S*)-configuration were found to be much more potent than the corresponding (*R*)-configured compounds **29** and **31**, which indicates (*S*)-methyl group was more suitable for the hydrophobic pocket

Table 3. SAR of Compounds with Selected Hinge Pieces

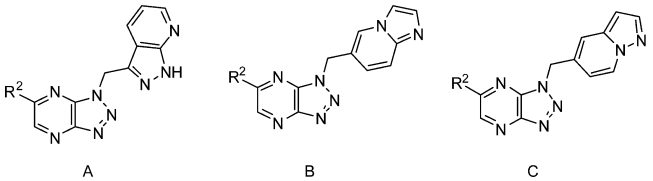

A B C

compound	R^2	IC_{50} [a] (μM)			MLM [b] Parent drug remaining(%)
		c-Met enzyme	p-Met	proliferation	
23A	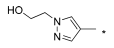	0.006	0.026	0.287	--[c]
23B	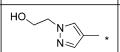	0.006	0.033	0.184	--[c]
23C	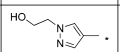	0.005	0.007	0.066	93.3
24A	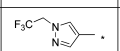	0.009	0.008	0.070	83.0
24B	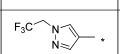	0.004	0.007	0.104	--[c]
24C	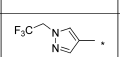	0.013	0.010	0.077	63.6
25B	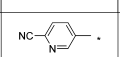	0.007	0.031	0.172	--[c]
25C	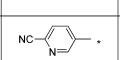	0.017	0.026	0.203	--[c]
26B	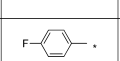	0.006	0.012	0.073	23.4
26C	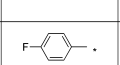	0.007	0.012	0.116	--[c]
27B	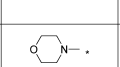	0.787	--[c]	--[c]	--[c]

[a] IC_{50}s are based on single runs of experiments. [b] Mouse liver microsome stability. [c] The -- indicates not tested.

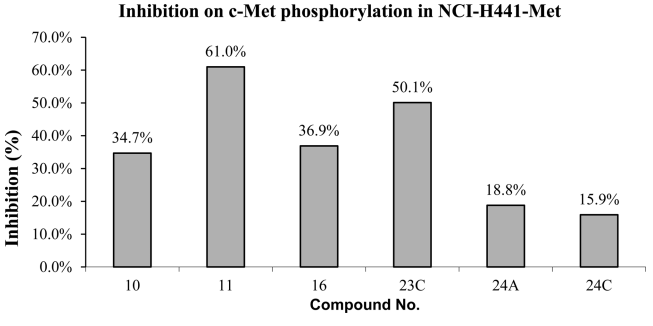

Figure 3. Inhibition on c-Met phosphorylation in NCI-H441. Experiments were carried out in female athymic mice (n = 4); po, 3 mg/kg (0.5% carboxymethyl cellulose (CMC), pH = 2.1).

dx.doi.org/10.1021/jm500510f | *J. Med. Chem.* 2014, 57, 7577−7589

Table 4. Pharmacokinetic Profiles of Selected Compounds in Mice[a]

compd	CL_{plasma}[b] (L/h·kg)	V_z[b] (L/kg)	$T_{1/2}$[c] (h)	C_{max}[c] (ng/mL)	AUC_{0-8h}[c] (ng·h/mL)	F_{oral}[c] (%)
16	4.28	5.4	1.3	1383	1067	46
23C	1.29	2.4	3.7	1920	7004	90.8

[a]Experiments were carried out in male ICR mice (n = 3). Dose: iv, 2.5 mg/kg (0.25% DMSO, 10% solutol, 10% ethanol, and 79.75% saline); po, 14.1 mg/kg (0.5% CMC, pH = 2.1). [b]Parameters obtained after iv dosing. [c]Parameters obtained after po dosing.

Table 5. SAR of [1,2,3]Triazolo[4,5-*b*]pyrazine Scaffold

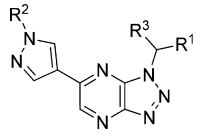

compound	R^1	R^2	R^3	IC_{50}[a] (μM)		
				c-Met enzyme	p-Met	proliferation
28		Me	(*S*)-Me	0.005	0.003	0.006
29		Me	(*R*)-Me	0.032	0.032	0.113
30		CH_2CH_2OH	(*S*)-Me	0.007	0.003	0.016
31		CH_2CH_2OH	(*R*)-Me	0.030	0.027	0.165

[a]IC_{50S} are based on single runs of experiments except for compound **28**'s c-Met enzyme and p-Met (n = 3).

Given its very potent c-Met activities, compound **28** was evaluated in vivo in a mouse pharmacokinetic study (Table 6). It demonstrated a much more desired pharmacokinetic profile in mice compared to the nonmethyl compound **16**, suggesting that the methyl helps to block a potential metabolic site as we originally designed. The clearance was reduced to 0.66 L/(h·kg) from 4.28 L/(h·kg), and the half-time was slightly enhanced to 1.7 h from 1.3 h. Despite the moderate oral bioavailability, the overall plasma exposure was much higher.

On the basis of the high systemic exposures, compound **28**'s inhibition of HGF-mediated c-Met phosphorylation in mice was evaluated. **28** demonstrated 84.7% inhibition at 6 h after a single oral dose of 3 mg/kg, much better than the 36.9% inhibition observed with **16** at 3 mg/kg.

Encouraged by the desired PK profile and sustainable in vivo target inhibition for at least 6 h, compound **28** was further evaluated for its in vivo efficacy in U87MG subcutaneous xenograft model in athymic nude mice. The compound was administered orally once a day at various dose levels for 21 days.

As shown in Figure 4, compound **28** demonstrated dose-dependent tumor growth inhibition in a U87MG subcutaneous xenograft model. The percent tumor growth inhibition (%TGI) at day 21 was 52.8%, 76.6% ,and 92.8% at 1, 2.5, and 10.0 mg/kg, respectively. In addition, none of the mice in the dosing groups exhibited body weight loss during the experiment.

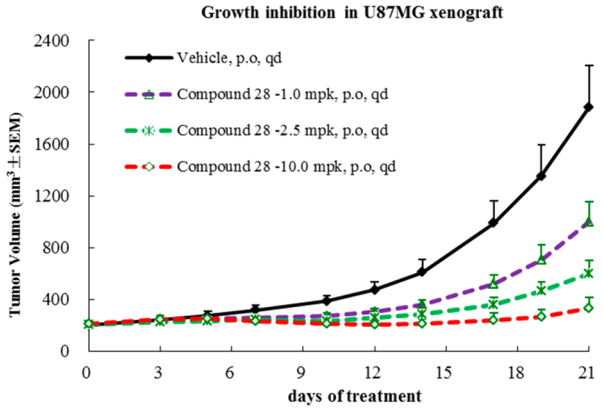

Figure 4. Growth inhibition of **28** in U87MG xenograft model in mice.

As mentioned earlier, one potential hypothesis for the toxicity seen in the known second generation c-Met inhibitors is that it arises from the insoluble products of AO metabolism. A metabolic study revealed that AO-mediated oxidization of compound **28** mainly took place on the central core of compound **28**, generating a relatively polar metabolite **28-AO** (Figure 5). **28-AO**'s solubility in aqueous buffers is 0.02 (pH 7.4) and 20.9 mg/mL (pH 1.2), comparable to compound **28**'s 0.02 and 31.8 mg/mL, respectively. Importantly, after being co-incubated with and without NADPH in human liver S9 fractions at 37 °C water bath for 60 min, the relative amounts of **28** are 99.08% and 99.66% estimated by the peak intensity of ultraviolet detection at 348 nm, and **28-AO** were only 0.22% and 0.34%, respectively. We therefore think the AO metabolism will not be significant for compound **28**, and in any case since the solubility of the resulting metabolite is comparable to the parent, AO metabolism should not lead to a safety concern in humans.[18]

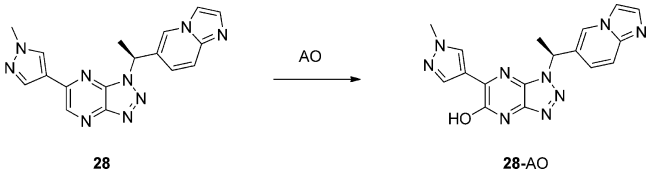

28 **28-AO**

Figure 5. AO metabolism of **28**.

Table 6. Pharmacokinetic Profile of 28[a]

compd	CL_{plasma}[b] (L/h·kg)	V_z[b] (L/kg)	$T_{1/2}$[c] (h)	C_{max}[c] (ng/mL)	AUC_{0-8h}[c] (ng·h/mL)	F_{oral}[c] (%)
28	0.66	1.2	1.7	4947	5594	27.2

[a]The experiments was carried out in male ICR mice (n = 3). Dose: iv, 2.5 mg/kg (0.25% DMSO, 10% solutol, 10% ethanol, and 79.75% saline); po, 10 mg/kg (0.5% CMC, pH = 2.1). [b]Parameters obtained after iv dosing. [c]Parameters obtained after po dosing.

dx.doi.org/10.1021/jm500510f | J. Med. Chem. 2014, 57, 7577−7589

Scheme 1. Synthesis of 2 and 3[a]

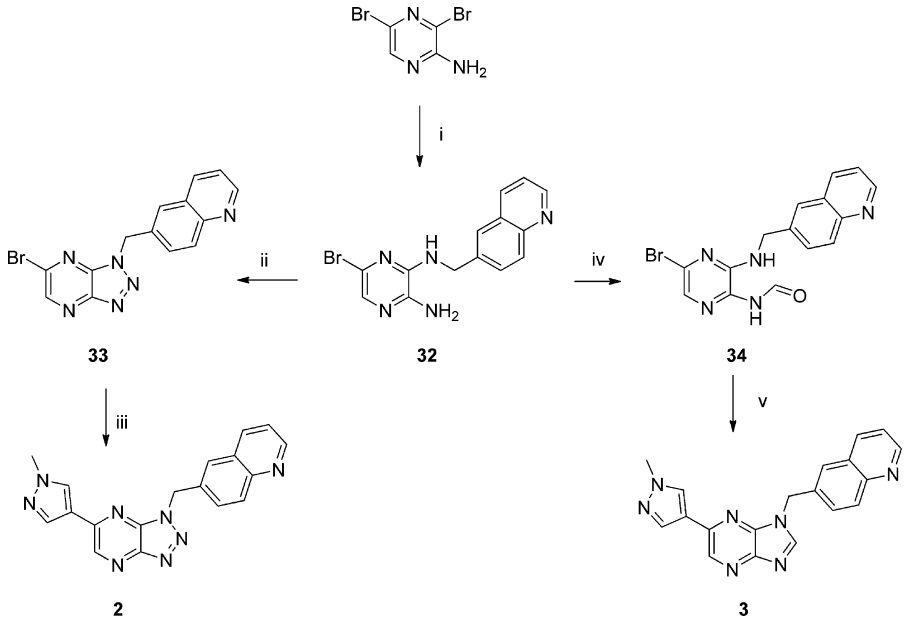

[a]Reagents and conditions: (i) DIEA, 130 °C; (ii) $NaNO_2$, acetic acid (AcOH), H_2O, H_2SO_4, rt; (iii) Pd(dppf)Cl_2, Cs_2CO_3, dioxane, H_2O, 110 °C; (iv) trimethoxymethane, 120 °C; (v) Pd(dppf)Cl_2, $NaHCO_3$, DME, H_2O, N_2, 110 °C, microwave.

When tested against a panel of diverse kinases, compound **28** exhibited exquisite selectivity for c-Met over 274 kinases.

Chemistry. Outlined in Scheme 1 is the synthesis of compounds **2** and **3**. A reaction of 3,5-dibromopyrazin-2-amine with quinolin-6-ylmethanamine in the presence of *N*,*N*-diisopropylethylamine (DIEA) afforded intermediate **32.** Subsequently **32** was treated with $NaNO_2$ under acidic conditions to give **33**, followed by Suzuki coupling with 1-methyl-4-(4,4,5,5-tetramethyl-1,3,2-dioxaborolan-2-yl)-1*H*-pyrazole to provide compound **2**. When **32** reacted with trimethoxymethane, **34** was obtained, which was subjected to intramolecular cyclization and Suzuki−Miyaura cross-coupling to produce compound **3**.

Preparation of compound **4** was accomplished in a similar manner to **2** using the corresponding intermediate **35**, which was prepared from the reductive amination of 5-bromopyridine-2,3-diamine and quinoline-6-carbaldehyde (Scheme 2).

Scheme 2. Synthesis of 4a[a]

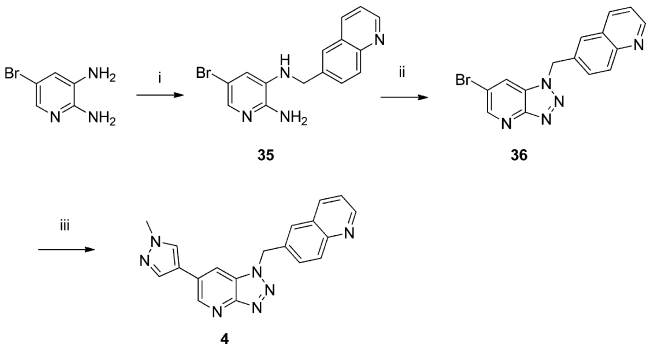

[a]Reagents and conditions: (i) quinoline-6-carbaldehyde, AcOH, MeOH, then $NaBH(AcO)_3$, rt; (ii) $NaNO_2$, AcOH, H_2O, H_2SO_4, rt; (iii) Pd(dppf)Cl_2, Cs_2CO_3, dioxane, H_2O, 110 °C.

The synthesis of **5**−**7** is described in Scheme 3. The chlorine of **37** was substituted with quinolin-6-ylmethanamine to give **38**, followed by the reduction of NO_2 to **39**. **39** was utilized to construct **5**−**7** as the similar procedures of **2** and **3**.

Compounds **9**-**27B** and **43**-**44** were synthesized according to the general process as depicted in Scheme 4. Treatment of 3,5-dibromopyrazin-2-amine with the corresponding amines under basic conditions yielded intermediates **41**. Diazotization and subsequent intramolecular cyclization of **41** afforded **42**. The palladium-catalyzed coupling of bromide **42** with the corresponding boric esters gave the desired compounds **9**-**26C** and **43**-**44**. The substitution of bromine by morpholine in the presence of K_2CO_3 provided **27B**.

Scheme 5 shows compounds **28** and **29** were isolated from racemic compounds **43** by HPLC, and compounds **30** and **31** were separated from the corresponding racemic compounds **44** by HPLC.

CONCLUSIONS

In conclusion, a series of novel, highly potent, and selective c-Met tyrosine kinase inhibitors with new hinge piece moieties were successfully designed and synthesized. These compounds are structurally differentiated from known compounds with toxicity liabilities. Among them, the most promising compound, **28**, has exquisite kinase selectivity and excellent potency and showed dose-dependent antitumor efficacy in vivo. Compound **28**, Volitinib, is now in phase Ib/II clinical development for treatment of cancer.[19−24]

EXPERIMENTAL SECTION

All reagents and solvents employed were purchased commercially and used without further Centigrade, and pressure is at or near atmospheric. NMR data were recorded on a Varian 400-MR machine. Chemical shifts are expressed as δ units using tetramethylsilane as the external standard (in NMR description, s, singlet; d, doublet; t, triplet; q, quartet; m, multiplet; and br, broad peak). All coupling constants (J) are reported in Hertz. MS data were checked by agilent 6120 or

dx.doi.org/10.1021/jm500510f | J. Med. Chem. 2014, 57, 7577−7589

Scheme 3. Synthesis of 5−7[a]

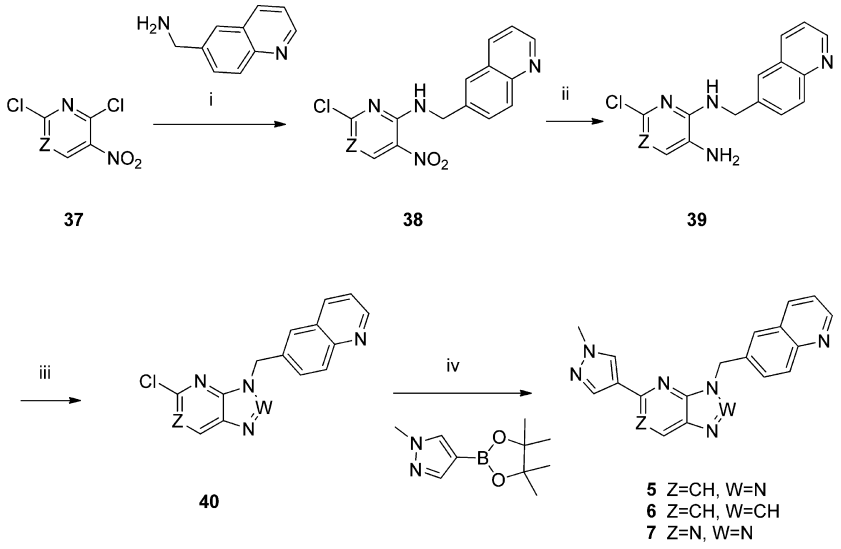

[a]Reagents and conditions: **5**: (i) Na_2CO_3, *i*-PrOH, rt; (ii) Pd/C, H_2, EtOAc (ethyl acetate), rt; (iii) Pd(dppf)Cl_2, Cs_2CO_3, dioxane, H_2O, 110 °C. **6**: (i) Na_2CO_3, *i*-PrOH, rt; (ii) Pd/C, H_2, EtOAc, rt; (iii) trimethoxymethane, *p*-TsOH, 120 °C, N_2; (iv) Pd(dppf)Cl_2, Cs_2CO_3, dioxane, H_2O, 100 °C. **7**: (i) Na_2CO_3, EtOAc, rt; (ii) $SnCl_2.2H_2O$, MeOH, 1,2-dichloroethane, 60 °C; (iii) $NaNO_2$, AcOH, H_2SO_4, H_2O; (iv) $Pd_2(dba)_3$, P(*t*-Bu)HBF_4, dioxane, H_2O, 100 °C, N_2.

Scheme 4. Synthesis of 9-27B and 43-44[a]

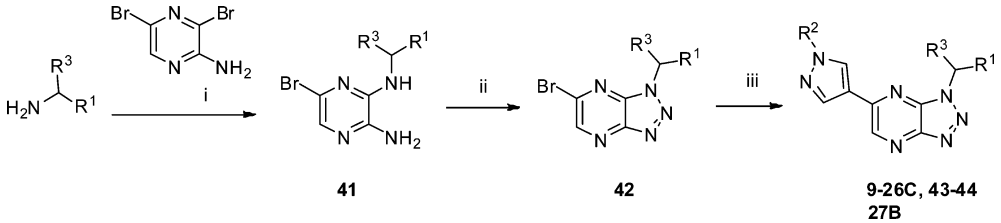

[a]Reagents and conditions: (i) DIEA or other bases, 100−150 °C; (ii) $NaNO_2$, AcOH, H_2O, H_2SO_4, rt; **9-26C**, **43-44**: (iii) 1-methyl-4-(4,4,5,5-tetramethyl-1,3,2-dioxaborolan-2-yl)-1H-pyrazole, Pd(dppf)Cl_2, Cs_2CO_3 or other bases, dioxane, or DME, H_2O, 100−110 °C. **27B**: (iii): morpholine, K_2CO_3, *N*,*N*-dimethylformamide, rt.

Scheme 5. Preparation of 28-31

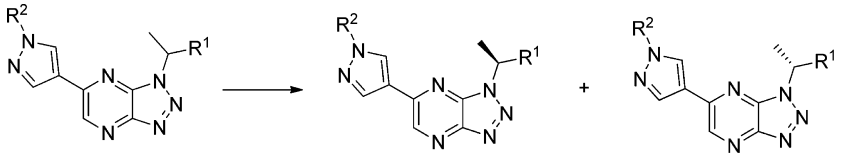

agilent 1100. Mass spectra were measured with an Agilent quadrupole 6110 spectrometer using an ESI+APCI source coupled to an Agilent 1200 HPLC system or an 1100 series LC/MSD trap spectrometer using an ESI source coupled to an Agilent 1100 HPLC system. IC_{50} values were calculated using XL-Fit 2.0 software. Unless indicated otherwise, compound purity was determined by HPLC with a confirming purity of ≥95% for all final biological testing compounds. HPLC method: Aglilent 1200 HPLC, Column:ymc AQ C18 150 × 4.6 cm 5u; Mobile phase: H_2O (0.1% formic acid) and MeOH(0.1% formic acid); Gradient: 5% MeOH in 0−10 min, 95% MeOH in 10−13 min, 5% MeOH in 13−14 min; Flow rate: 1 mL/min; Detector: 254 nm.

Preparation of 6-((6-(1-methyl-1*H*-pyrazol-4-yl)-1*H*-[1,2,3]-triazolo[4,5-*b*]pyrazin-1-yl)methyl)quinoline (2). The mixture of quinolin-6-ylmethanamine (727 mg, 4.6 mmol), 3,5-dibromopyrazin-2-amine (1160 mg, 4.6 mmol) and DIEA (669 mg, 5.2 mmol) was stirred overnight at 130 °C in a sealed tube. The reaction mixture was concentrated and recrystallized with EtOAc to afford **32** as a yellow solid (1.25 g, 82%). MS (*m*/*z*): 332 $(M + 1)^+$.

To a solution of **32** (500 mg, 1.51 mmol) in 4 mL of H_2O was added AcOH (4 mL), followed by a solution of $NaNO_2$ (125 mg, 1.81 mmol) in water (1 mL) dropwise at 0 °C. The mixture was stirred at 0 °C for 1.5 h, then added aq. H_2SO_4 (50%, 0.5 mL), and stirred at rt for another 1.5 h. The second batch of aq. H_2SO_4 (50%, 0.5 mL) was added, followed by a solution of $NaNO_2$ (30 mg, 0.43 mmol) in water (1 mL) dropwise, and stirred at rt for 1 h. The reaction mixture was adjusted to pH ∼ 8 with aq. NaOH (20%) and extracted with EtOAc. The organic layers were dried over $MgSO_4$ and concentrated to afford **33** as a yellow solid (200 mg), which was used directly for the next step. MS (*m*/*z*): 341 $(M + 1)^+$.

dx.doi.org/10.1021/jm500510f | *J. Med. Chem.* 2014, 57, 7577−7589

To a solution of crude **33** (50 mg, 0.15 mmol) in 5 mL of dioxane and 0.5 mL of H_2O were added 1-methyl-4-(4,4,5,5-tetramethyl-1,3,2-dioxaborolan-2-yl)-1*H*-pyrazole (45 mg, 0.32 mmol), pd(dppf)Cl_2 (12 mg, 0.015 mmol), and Cs_2CO_3 (143 mg, 0.45 mmol). The reaction was stirred at 110 °C overnight under N_2. The reaction mixture was concentrated and purified by flash column chromatography to afford **2** as a light-yellow solid (40 mg, 80%). Purity: 96.7%, RT 8.21. MS (*m*/*z*): 343 $(M + 1)^+$. ^1H NMR (400 MHz, DMSO-d_6) δ 9.22 (s, 1H), 8.90 (dd, *J* = 4.1, 1.5 Hz, 1H), 8.65 (s, 1H), 8.38 (d, *J* = 7.7 Hz, 1H), 8.31 (s, 1H), 8.04 (d, *J* = 8.7 Hz, 1H), 8.01 (s, 1H), 7.84 (dd, *J* = 8.6, 1.9 Hz, 1H), 7.54 (dd, *J* = 8.3, 4.2 Hz, 1H), 6.16 (s, 2H), 3.95 (s, 3H).

Preparation of 6-((6-(1-methyl-1*H*-pyrazol-4-yl)-*1H*-imidazo-[4,5-*b*]pyrazin-1-yl)methyl)quinoline (3). A mixture of **32** (66 mg, 0.2 mmol) and trimethoxymethane (1 mL) was stirred at 120 °C for 3 h. The reaction mixture was concentrated, and the resulting residue was dissolved in toluene and stirred at reflux for 18 h, then concentrated, and used directly for the next step. MS (*m*/*z*): 359.5 $(M + 1)^+$.

The crude intermediate above (36 mg, 0.10 mmol), 1-methyl-4-(4,4,5,5-tetramethyl-1,3,2-dioxaborolan-2-yl)-1*H*-pyrazole (22 mg, 0.11 mol), Pd(dppf)Cl_2 (7 mg, 0.01 mmol), and $NaHCO_3$ (16 mg, 0.20 mmol) were dissolved in DME (1 mL) and H_2O (0.2 mL), the resulting mixture was bubbled with N_2 for a while, then stirred at 110 °C under microwave condition for 40 min. The reaction mixture was concentrated and purified by flash column chromatography to afford **3** as a white solid (6 mg, 17%). Purity: 99.6%, RT 7.94. MS (*m*/*z*): 342 $(M + 1)^+$. ^1H NMR (400 MHz, DMSO-d_6) δ 8.89−8.87 (m, 3H), 8.41 (s, 1H), 8.36 (d, *J* = 8.0 Hz, 1H), 8.13 (s, 1H), 8.02 (d, *J* = 8.8 Hz, 1H), 7.98 (d, *J* = 1.6 Hz, 1H), 7.85 (dd, *J* = 8.8, 2.0 Hz, 1H), 7.52 (dd, *J* = 8.4, 4.0 Hz, 1H), 5.73 (s, 2H), 3.91 (s, 3H).

Preparation of 6-((6-(1-methyl-1*H*-pyrazol-4-yl)-1*H*-[1,2,3]-triazolo[4,5-*b*]pyridin-1-yl)methyl)quinoline (4). To a solution of 5-bromopyridine-2,3-diamine (188 mg, 1 mmol) and quinoline-6-carbaldehyde (157 mg, 1 mmol) in MeOH (5 mL) was added 4 drops of CH_3COOH, the reaction was stirred at rt for 2 h, then added $NaBH(AcO)_3$ (414 mg, 2 mmol), and stirred at rt for 16 h. The reaction mixture was concentrated and purified by column chromatography to afford **35** (329 mg).

Compound **4** was prepared in a similar manner as compound **2** using **35** as a starting material instead of **32**. Purity: 95.1%, RT 8.54. MS (*m*/*z*): 342 $(M + 1)^+$. ^1H NMR (400 MHz, CD_3OD) δ 9.00 (d, *J* = 2.0 Hz, 1H), 8.84 (dd, *J* = 4.4, 1.6 Hz,, 1H), 8.57 (d, *J* = 1.6 Hz, 1H), 8.36 (d, *J* = 8.0.Hz, 1H), 8.17 (s, 1H), 8.02−7.98 (m, 3H), 7.86 (dd, *J* = 8.4, 2.0 Hz, 1H), 7.56 (dd, *J* = 8.4, 4.4 Hz, 1H), 6.18 (s, 2H), 3.93 (s, 3H).

Preparation of 6-((5-(1-methyl-1*H*-pyrazol-4-yl)-3*H*-[1,2,3]-triazolo[4,5-*b*]pyridin-3-yl)methyl)quinoline (5). To a solution of quinolin-6-ylmethanamine (158 mg, 1 mmol) in 5 mL of *i*-PrOH were added 2,6-dichloro-3-nitropyridine (193 mg, 1 mmol), and Na_2CO_3 (318 mg, 3 mmol), the reaction was stirred at rt overnight. The reaction mixture was concentrated. The resulting residue was diluted with EtOAc (50 mL) and washed with water and conc. NH_4Cl solution (15 mL). The organic layers were dried over anhydrous $MgSO_4$ and concentrated to afford the crude product **38** (Z = CH) as a yellow solid (300 mg). MS (*m*/*z*): 316 $(M + 1)^+$.

The mixture of crude **38** (Z = CH) (250 mg, 0.8 mmol) and Pd/C (10%, 200 mg) in EtOAc (30 mL) was stirred at rt under H_2 for 4 h. The reaction mixture was filtered, concentrated, and purified by column chromatography to afford **39** (Z = CH) as a yellow solid (130 mg, 57%). MS (*m*/*z*): 286 $(M + 1)^+$.

Compound **5** was prepared in a similar manner as compound **2** using **39** (Z = CH) as a starting material instead of **32**. Purity: 100%, RT 8.76. MS (*m*/*z*): 342 $(M + 1)^+$. ^1H NMR (400 MHz, DMSO-d_6) δ 8.89 (s, 1H), 8.59−8.44 (m, 2H), 8.38 (d, *J* = 8.2 Hz, 1H), 8.19 (s, 1H), 8.07−7.97 (m, 2H), 7.88−7.74 (m, 2H), 7.53 (dd, *J* = 8.1, 3.9 Hz, 1H), 6.12 (s, 2H), 3.92 (s, 3H).

Preparation of 6-((5-(1-methyl-1*H*-pyrazol-4-yl)-3*H*-imidazo-[4,5-*b*]pyridin-3-yl)methyl)quinoline (6). A mixture of **39** (Z = CH) (142 mg, 0.5 mmol), trimethoxymethane (5 mL), and *p*-TsOH (45 mg, 0.25 mmol) was stirred at 120 °C under N_2 for 2 h. The reaction mixture was concentrated and purified by chromatography to afford **40** (Z, W = CH) (143 mg, 96.6%). MS (*m*/*z*): 295 $(M + 1)^+$.

A mixture of **40** (Z, W = CH) (58 mg, 0.2 mmol), 1-methyl-4-(4,4,5,5-tetramethyl-1,3,2-dioxaborolan-2-yl)-1*H*-pyrazole (82 mg, 0.4 mmol), and Cs_2CO_3 (192 mg, 0.6 mmol) in dioxane (5 mL) and H_2O (0.5 mL) was heated to 100 °C, then added Pd(dppf)Cl_2 (32 mg, 0.04 mmol), and the reaction was stirred at 100 °C under N_2 overnight. After cooling to rt, the reaction mixture was concentrated and purified by flash column chromatography to afford **6** (10 mg, 6%). Purity: 98.8%, RT 8.09. MS (*m*/*z*): 341 $(M + 1)^+$. ^1H NMR (400 MHz, DMSO-d_6) δ 8.85 (dd, *J* = 4.0, 1.6 Hz, 1H), 8.56 (s, 1H), 8.34 (d, *J* = 7.2 Hz, 1H), 8.27 (s, 1H), 8.04−7.98 (m, 4H), 7.85 (dd, *J* = 8.4, 2.0 Hz, 1H), 7.56 (d, *J* = 8.4 Hz, 1H), 7.54 (dd, *J* = 8.4, 4.0 Hz, 1H), 5.69 (s, 2H), 3.87 (s, 3H).

Preparation of 6-((5-(1-methyl-1*H*-pyrazol-4-yl)-3*H*-[1,2,3]-triazolo[4,5-*d*]pyrimidin-3-yl)methyl)quinoline (7). Compound **7** was prepared by a procedure similar to that described for the synthesis of compound **5** using 2,4-dichloro-5-nitropyrimidine as a starting material instead of 2,6-dichloro-3-nitropyridine. Purity: 98.2%, RT 8.61. MS (*m*/*z*): 343 $(M + 1)^+$. ^1H NMR (400 MHz, DMSO-d_6) δ 9.70 (s, 1H), 8.91 (dd, *J* = 4.0, 2.0 Hz, 1H), 8.53 (s, 1H), 8.39 (d, *J* = 6.8 Hz, 1H), 8.17 (d, *J* = 0.8 Hz, 1H), 8.05 (d, *J* = 8.4 Hz,1H), 8.00(d, *J* = 1.6 Hz,1H), 7.84 (dd, *J* = 8.4, 2.0 Hz, 1H), 7.56 (dd, *J* = 8.0, 4.0 Hz, 1H), 6.13 (s, 2H), 3.94 (s, 3H).

Preparation of 6-((6-(1-methyl-1*H*-pyrazol-4-yl)-[1,2,4]-triazolo[4,3-*b*]pyridazin-3-yl)methyl)quinolone (8).[25] The title compound was prepared similar to the reference WO2007/138472. Purity: 98.1%, RT 7.76. MS (*m*/*z*): 342 $(M + 1)^+$. ^1H NMR (400 MHz, DMSO-d_6) δ 8.84 (d, *J* = 2.8 Hz, 1H), 8.56 (s, 1H), 8.35−8.31 (m, 2H), 8.16 (s, 1H),7.98−7.96 (m, 2H), 7.82−7.80 (m, 1H), 7.68 (d, *J* = 9.6 Hz Hz, 1H), 7.51−7.48 (m, 1H), 4.73 (s, 2H), 3.93 (s, 3H).

Compounds **9**-**27B** and **43**-**44** were prepared by a procedure similar to that described for the synthesis of compound **2** using the corresponding amines instead of quinolin-6-ylmethanamine.

2-(4-(1-((1*H*-pyrrolo[2,3-*b*]pyridin-2-yl)methyl)-1*H*-[1,2,3]-triazolo[4,5-*b*]pyrazin-6-yl)-1*H*-pyrazol-1-yl)ethanol (9). Purity: 96.8%, RT 8.09. MS (*m*/*z*): 362 $(M + 1)^+$. ^1H NMR (400 MHz, DMSO-d_6) δ 11.89 (s, 1H), 9.23 (s, 1H), 8.63 (s, 1H), 8.37 (br, 1H), 8.31 (s, 1H), 8.19 (d, *J* = 6.4 Hz, 1H), 7.89 (d, *J* = 8.0 Hz, 1H), 7.05−7.02 (m, 1H), 6.44 (s, 1H), 6.09 (s, 2H), 4.26−4.23(m, 2H), 3.81−3.77 (m, 2H).

2-(4-(1-((1*H*-pyrrolo[2,3-*b*]pyridin-3-yl)methyl)-1*H*-[1,2,3]-triazolo[4,5-*b*]pyrazin-6-yl)-1*H*-pyrazol-1-yl)ethanol (10). Purity: 99.8%, RT 8.20. MS (*m*/*z*): 362 $(M + 1)^+$. ^1H NMR (400 MHz, DMSO-d_6) δ 11.77 (s, 1H), 9.18 (s, 1H), 8.68 (s, 1H), 8.35 (s, 1H), 8.20 (d, *J* = 4.8 Hz, 1H), 8.15 (d, *J* = 8.0 Hz, 1H), 7.79−7.76 (m, 1H), 7.36 (br, 1H), 7.24 (br, 1H), 7.12−7.07 (m, 2H), 6.06 (s, 2H), 5.04 (t, *J* = 4.8 Hz, 1H), 4.27 (t, *J* = 5.2 Hz, 2H), 3.84−3.79 (m, 2H).

1-((1*H*-pyrazolo[3,4-*b*]pyridin-3-yl)methyl)-6-(1-methyl-1*H*-pyrazol-4-yl)-1*H*-[1,2,3]triazolo[4,5-*b*]pyrazine (11). Purity: 99.0%, RT 8.86. MS (*m*/*z*): 333 $(M + 1)^+$. ^1H NMR (400 MHz, DMSO-d_6) δ 9.17 (s, 1H), 8.61 (s, 1H), 8.52 (dd, *J* = 4.4, 2.0 Hz,1H), 8.44 (br, 1H), 8.33 (dd, *J* = 8.4, 2.0 Hz, 1H), 8.25 (s, 1H), 7.23 (dd, *J* = 8.0, 4.4 Hz, 1H), 6.26 (s, 2H), 3.93 (s, 3H).

3-((6-(1-methyl-1*H*-pyrazol-4-yl)-1*H*-[1,2,3]triazolo[4,5-*b*]-pyrazin-1-yl)methyl)thieno[2,3-*b*]pyridine (12). Purity: 95.2%, RT 9.72. MS (*m*/*z*): 349 $(M + 1)^+$. ^1H NMR (400 MHz, DMSO-d_6) δ 9.18 (s, 1H), 8.65 (s, 1H), 8.60 (dd, *J* = 4.8, 1.6 Hz, 1H), 8.50 (dd, *J* = 8.0, 1.6 Hz, 1H), 8.31 (d, *J* = 0.4 Hz, 1H), 8.07 (s, 1H), 7.53 (dd, *J* = 8.0, 4.4 Hz, 1H), 6.21 (s, 2H), 3.96 (s, 3H).

2-((6-(1-methyl-1*H*-pyrazol-4-yl)-1*H*-[1,2,3]triazolo[4,5-*b*]-pyrazin-1-yl)methyl) thieno[2,3-*b*]pyridine (13). Purity: 99.0%, RT 9.75. MS (*m*/*z*): 349 $(M + 1)^+$. ^1H NMR (400 MHz, DMSO-d_6) δ 9.23 (s, 1H), 8.66 (s, 1H), 8.53 (d, *J* = 3.2 Hz, 1H), 8.32 (s, 1H), 8.25 (d, *J* = 8.0 Hz, 1H), 7.58 (s, 1H), 7.44 (dd, *J* = 8.0, 4.8 Hz, 1H), 6.30 (s, 2H), 3.97 (s, 3H).

2-((6-(1-methyl-1*H*-pyrazol-4-yl)-1*H*-[1,2,3]triazolo[4,5-*b*]-pyrazin-1-yl)methyl) thieno[3,2-*c*]pyridine (14). Purity: 100%, RT 6.98. MS (*m*/*z*): 348 $(M)^+$. ^1H NMR (400 MHz, DMSO-d_6) δ 9.23 (s, 1H), 9.09 (s, 1H), 8.65 (s, 1H), 8.40 (d, *J* = 5.5 Hz, 1H), 8.32

(s, 1H), 8.00 (d, J = 5.6 Hz, 1H), 7.73 (s, 1H), 6.32 (s, 2H), 3.96 (s, 3H).

5-((6-(1-methyl-1*H*-pyrazol-4-yl)-1*H*-[1,2,3]triazolo[4,5-*b*]-pyrazin-1-yl)methyl)-1*H*-thieno[3,2-*c*]pyrazole (15). Purity: 98.1%, RT 9.18. MS (m/z): 338 (M + 1)$^+$. ^{1}H NMR (400 MHz, CD_3OD) δ 9.06 (s, 1H), 8.47 (s, 1H), 8.26 (s, 1H), 7.71 (s, 1H), 7.31 (s, 1H), 6.15 (d, J = 0.8 Hz, 2H), 3.99 (s, 3H).

1-(imidazo[1,2-*a*]pyridin-6-ylmethyl)-6-(1-methyl-1*H*-pyrazol-4-yl)-1*H*-[1,2,3]triazolo[4,5-*b*]pyrazine (16). Purity: 97.6%, RT 6.35. MS (m/z): 332 (M + 1)$^+$. ^{1}H NMR (400 MHz, DMSO-d_6) δ 9.20 (d, J = 0.8 Hz, 1H), 8.76 (d, J = 0.8 Hz, 1H), 8.65 (s, 1H), 8.32 (s, 1H), 7.99 (s, 1H), 7.58−7.55 (m, 2H), 7.33 (dd, J = 9.2, 1.2 Hz, 1H), 5.96 (s, 2H), 3.96 (s, 3H).

1-(imidazo[1,2-*a*]pyrazin-6-ylmethyl)-6-(1-methyl-1*H*-pyrazol-4-yl)-1*H*-[1,2,3]triazolo[4,5-*b*]pyrazine (17). Purity: 98.5%, RT 8.07. MS (m/z): 333(M + 1)$^+$. ^{1}H NMR (400 MHz, DMSO-d_6) δ 9.17 (s, 1H), 8.96 (s, 1H), 8.84 (s, 1H), 8.59 (s, 1H), 8.23 (s, 1H), 8.19 (s, 1H), 7.83 (s, 1H), 6.00 (s, 2H), 3.91 (s, 3H).

1-([1,2,4]triazolo[1,5-*a*]pyridin-6-ylmethyl)-6-(1-methyl-1*H*-pyrazol-4-yl)-1*H*-[1,2,3]triazolo[4,5-*b*]pyrazine (18). Purity: 99.9%, RT 8.67. MS (m/z): 333 (M + 1)$^+$. ^{1}H NMR (400 MHz, DMSO-d_6) δ 9.26 (s, 1H), 9.19 (s, 1H), 8.65 (s, 1H), 8.53 (s, 1H), 8.30 (s, 1H), 7.86 (d, J = 9.2 Hz, 1H), 7.77 (dd, J = 9.2, 1.7 Hz, 1H), 6.07 (s, 2H), 3.96 (s, 3H).

1-(imidazo[1,2-*b*]pyridazin-6-ylmethyl)-6-(1-methyl-1*H*-pyrazol-4-yl)-1*H*-[1,2,3]triazolo[4,5-*b*]pyrazine (19). Purity: 98.8%, RT 7.42. MS (m/z): 333 (M + 1)$^+$. ^{1}H NMR (400 MHz, CD_3OD) δ 9.08 (s, 1H), 8.43 (s, 1H), 8.21 (s, 1H), 8.04−8.00 (m, 2H), 7.72 (s, 1H), 7.40 (d, J = 9.2 Hz, 1H), 6.21 (s, 2H), 3.97 (s, 3H).

6-(1-methyl-1*H*-pyrazol-4-yl)-1-(pyrazolo[1,5-*a*]pyridin-5-ylmethyl)-1*H*-[1,2,3]triazolo[4,5-*b*]pyrazine (20). Purity: 98.1%, RT 9.42. MS (m/z): 332 (M + 1)$^+$. ^{1}H NMR (400 MHz, DMSO-d_6) δ 9.19 (s, 1H), 8.65−8.63 (m, 2H), 8.27 (s, 1H), 7.96 (d, J = 2.4 Hz, 1H), 7.65 (s, 1H), 6.88 (dd, J = 7.2, 2.0 Hz, 1H), 6.58 (d, J = 1.6 Hz, 1H), 5.96 (s, 2H), 3.92 (s, 3H).

6-(1-methyl-1*H*-pyrazol-4-yl)-1-(pyrazolo[1,5-*a*]pyrimidin-5-ylmethyl)-1*H*-[1,2,3]triazolo[4,5-*b*]pyrazine (21). Purity: 95.5%, RT 8.66. MS (m/z): 333 (M + 1)$^+$. ^{1}H NMR (400 MHz, CD_3OD) δ 9.10 (s, 1H), 8.91(dd, J = 7.2, 0.8 Hz, 1H), 8.43 (s, 1H), 8.21 (d, J = 0.4 Hz, 1H), 8.11 (d, J = 2.4 Hz, 1H), 7.08 (d, J = 7.2 Hz, 1H), 6.54 (dd, J = 2.4, 0.8 Hz, 1H), 6.18 (s, 2H), 3.96 (s, 3H).

1-([1,2,4]triazolo[1,5-*a*]pyridin-7-ylmethyl)-6-(1-methyl-1*H*-pyrazol-4-yl)-1*H*-[1,2,3]triazolo[4,5-*b*]pyrazine (22). Purity: 99.5%, RT 8.55. MS (m/z): 333 (M + 1)$^+$. ^{1}H NMR (400 MHz, DMSO-d_6) δ 9.20 (s, 1H), 8.94 (d, J = 7.2 Hz, 1H), 8.62 (s, 1H), 8.48 (s, 1H), 8.27 (s, 1H), 7.85 (s, 1H), 7.21 (d, J = 6.8 Hz, 1H), 6.10 (s, 2H), 3.92 (s, 3H).

2-(4-(1-((1*H*-pyrazolo[3,4-*b*]pyridin-3-yl)methyl)-1*H*-[1,2,3]-triazolo[4,5-*b*]pyrazin-6-yl)-1*H*-pyrazol-1-yl)ethanol (23A). Purity: 99.2%, RT 8.17. MS (m/z): 363 (M + 1)$^+$. ^{1}H NMR (400 MHz, DMSO-d_6) δ 9.20 (s, 1H), 8.61 (s, 1H), 8.53 (dd, J = 8.4, 4.4 Hz, 1H), 8.35 (dd, J = 8.0, 1.6 Hz, 1H), 8.28 (s, 1H), 7.25 (dd, J = 8.0, 4.4 Hz, 1H), 6.28(s, 2H), 4.25−4.23 (m, 2H), 3.80−3.77 (m, 2H).

2-(4-(1-(imidazo[1,2-*a*]pyridin-6-ylmethyl)-1*H*-[1,2,3]-triazolo[4,5-*b*]pyrazin-6-yl)-1*H*-pyrazol-1-yl)ethanol (23B). Purity: 100%, RT 5.74. MS (m/z): 362 (M + 1)$^+$. ^{1}H NMR (400 MHz, DMSO-d_6) δ 9.22 (s, 1H), 8.76 (s, 1H), 8.66 (s, 1H), 8.34 (s, 1H), 7.98 (s, 1H), 7.57−7.55 (m, 2H), 7.33−7.31 (dd, J = 9.2, 1.6 Hz, 1H), 5.97 (s, 2H), 5.01−4.98 (m, 1H), 4.27−4.24 (m, 2H), 3.83−3.78 (m, 2H).

2-(4-(1-(pyrazolo[1,5-*a*]pyridin-5-ylmethyl)-1*H*-[1,2,3]-triazolo[4,5-*b*]pyrazin-6-yl)-1*H*-pyrazol-1-yl)ethanol (23C). Purity: 99.2%, RT 8.85. MS (m/z): 362 (M + 1)$^+$. ^{1}H NMR (400 MHz, DMSO-d_6) δ 9.21 (s, 1H), 8.64 (d, J = 7.2 Hz, 1H), 8.61 (s, 1H), 8.30 (s, 1H), 7.97 (d, J = 2.4 Hz, 1H), 7.67 (s, 1H), 6.88 (dd, J = 7.2, 1.6 Hz, 1H), 6.59 (dd, J = 2.0, 0.8, 1H), 5.98 (s, 2H), 4.98 (t, J = 5.2 Hz, 1H), 4.23 (t, J = 5.6 Hz, 2H), 3.80−3.75 (m, 2H).

1-((1H-pyrazolo[3,4-*b*]pyridin-3-yl)methyl)-6-(1-(2,2,2-trifluoroethyl)-1*H*-pyrazol-4-yl)-1*H*-[1,2,3]triazolo[4,5-*b*]pyrazine (24A). Purity: 100%, RT 9.17. MS (m/z): 401 (M + 1)$^+$. ^{1}H NMR (400 MHz, DMSO-d_6) δ 9.24 (s, 1H), 8.76 (s, 1H), 8.52 (dd, J = 4.8, 1.6 Hz, 1H), 8.43 (s, 1H), 8.34 (dd, J = 8.4, 1.6 Hz, 1H), 7.23 (dd, J = 8.0, 4.4 Hz, 1H), 6.29 (s, 2H), 5.32−5.26 (m, 2H).

1-(imidazo[1,2-*a*]pyridin-6-ylmethyl)-6-(1-(2,2,2-trifluoroethyl)-1*H*-pyrazol-4-yl)-1*H*-[1,2,3]triazolo[4,5-*b*]pyrazine (24B). Purity: 100%, RT 6.72. MS (m/z): 400 (M + 1)$^+$. ^{1}H NMR (400 MHz, DMSO-d_6) δ 9.27 (s, 1H), 8.82 (s, 1H), 8.76 (s, 1H), 8.50 (s, 1H), 7.98 (s, 1H), 7.58−7.55 (m, 2H), 7.34 (d, J = 9.6 Hz, 1H), 5.99 (s, 2H), 5.34−5.28 (m, 2H).

1-(pyrazolo[1,5-*a*]pyridin-5-ylmethyl)-6-(1-(2,2,2-trifluoroethyl)-1*H*-pyrazol-4-yl)-1*H*-[1,2,3]triazolo[4,5-*b*]pyrazine (24C). Purity: 100%, RT 9.78. MS (m/z): 400 (M + 1)$^+$. ^{1}H NMR (400 MHz, DMSO-d_6) δ 9.29 (s, 1H), 8.81 (s, 1H), 8.68 (d, J = 6.8 Hz, 1H), 8.48 (s, 1H), 7.99 (d, J = 2.0 Hz, 1H), 7.69 (s, 1H), 6.92 (d, J = 7.2 Hz, 1H), 6.61 (d, J = 1.6 Hz, 1H), 6.02 (s, 2H), 5.35−5.28 (m, 2H).

5-(1-(imidazo[1,2-*a*]pyridin-6-ylmethyl)-1*H*-[1,2,3]triazolo-[4,5-*b*]pyrazin-6-yl)picolinonitrile (25B). Purity: 100%, RT 6.10. MS (m/z): 354 (M + 1)$^+$. ^{1}H NMR (400 MHz, DMSO-d_6) δ 9.67−9.65 (m, 2H), 8.93−8.92 (m, 1H), 8.84 (s, 1H), 8.32 (d, J = 8.4 Hz, 1H), 7.98 (s, 1H), 7.58−7.53 (m, 2H), 7.37−7.35 (m, 1H), 6.10 (s, 2H).

5-(1-(pyrazolo[1,5-*a*]pyridin-5-ylmethyl)-1*H*-[1,2,3]triazolo-[4,5-*b*]pyrazin-6-yl)picolinonitrile (25C). Purity: 97.7%, RT 9.2.MS (m/z): 354 (M + 1)$^+$. ^{1}H NMR (400 MHz, DMSO-d_6) δ 9.65−9.62(m, 2H), 8.81−8.88 (dd, J = 8.4, 2.0 Hz,1H), 8.65 (d, J = 7.2 Hz, 1H), 8.30 (d, J = 8.4 Hz, 1H), 7.97 (d, J = 2.4 Hz, 1H), 7.75 (s, 1H), 6.93 (dd, J = 7.2, 1.6 Hz, 1H), 6.59 (d, J = 1.6 Hz, 1H), 6.11 (s, 2H).

6-(4-fluorophenyl)-1-(imidazo[1,2-*a*]pyridin-6-ylmethyl)-1*H*-[1,2,3]triazolo[4,5-*b*]pyrazine (26B). Purity: 95.2%, RT 7.26. MS (m/z): 346 (M + 1)$^+$. ^{1}H NMR (400 MHz, DMSO-d_6) δ 9.50 (s, 1H), 8.79 (s, 1H), 8.42−8.39 (m, 2H), 7.98 (s, 1H), 7.58−7.56 (m, 2H), 7.49−7.44 (m, 2H), 7.36 (d, J = 10.0 Hz, 1H), 6.06 (s, 2H).

6-(4-fluorophenyl)-1-(pyrazolo[1,5-*a*]pyridin-5-ylmethyl)-1*H*-[1,2,3]triazolo[4,5-*b*]pyrazine (26C). Purity: 100%, RT 10.66. MS (m/z): 346 (M + 1)$^+$. ^{1}H NMR (400 MHz, DMSO-d_6) δ 9.27 (s, 1H), 8.78 (s, 1H), 8.67 (d, J = 7.2 Hz, 1H), 8.48 (d, J = 0.8 Hz, 1H), 7.99 (d, J = 2.4 Hz, 1H), 7.69 (d, J = 0.8 Hz, 1H), 6.92 (dd, J = 7.2, 1.6 Hz, 1H), 6.61 (dd, J = 2.4, 0.8 Hz, 1H), 6.01 (s, 2H), 5.63 (s, 2H).

4-(1-(imidazo[1,2-*a*]pyridin-6-ylmethyl)-1*H*-[1,2,3]triazolo-[4,5-*b*]pyrazin-6-yl)morpholine (27B). Purity: 100%, RT 5.82. MS (m/z): 337 (M + 1)$^+$. ^{1}H NMR (400 MHz, DMSO-d_6) δ 8.71 (s, 1H), 8.57 (s, 1H), 7.9972 (s, 1H), 7.58 (br, 2H), 7.27 (d, J = 10.4 Hz, 1H), 5.75 (s, 2H), 3.75−7.54 (m, 8H).

Preparation of (*S*)-1-(1-(imidazo[1,2-*a*]pyridin-6-yl)ethyl)-6-(1-methyl-1*H*-pyrazol-4-yl)-1*H*-[1,2,3]triazolo[4,5-*b*]pyrazine (28) and (*R*)-1-(1-(imidazo[1,2-*a*]pyridin-6-yl)ethyl)-6-(1-methyl-1*H*-pyrazol-4-yl)-1*H*-[1,2,3]triazolo[4,5-*b*]pyrazine (29). The racemic compound **43** (prepared by a procedure similar to that described for the synthesis of compound **2** using the corresponding 1-(imidazo[1,2-*a*]pyridin-6-yl)ethanamine instead of quinolin-6-ylmethanamine) was resolved by an outsourced service to produce the optically pure two enantiomers **28** and **29**. Compound **43:** Purity: 100%, RT 6.78. MS (m/z): 346 (M + 1)$^+$. ^{1}H NMR (400 MHz, DMSO-d_6) δ 9.17 (s, 1H), 8.80 (s, 1H), 8.65 (s, 1H), 8.29 (s, 1H), 7.98 (s, 1H), 7.57−7.54 (m, 2H), 7.38 (dd, J = 9.4, 1.8 Hz, 1H), 6.40 (q, J = 7.2 Hz, 1H), 3.94 (s, 3H), 2.17 (d, J = 7.2 Hz, 3H). Compound **28**: MS (m/z): 346 (M + 1)$^+$. ^{1}H NMR (400 MHz, DMSO-d_6) δ 9.18 (s, 1H), 8.79 (s, 1H), 8.64 (s, 1H), 8.30 (s, 1H), 7.98 (s, 1H), 7.58−7.54 (m, 2H), 7.38 (dd, J = 9.2, 1.6 Hz, 1H), 6.42 (q, J = 7.2 Hz, 1H), 3.95 (s, 3H), 2.17 (d, J = 7.2 Hz, 3H). Purity: 99.9%, RT 15.07. ee: 100%. Compound **29**: MS (m/z): 346 (M + 1)$^+$. ^{1}H NMR (400 MHz, DMSO-d_6) δ 9.18 (s, 1H), 8.79 (s, 1H), 8.63 (s, 1H), 8.30 (s, 1H), 7.97 (s, 1H), 7.58−7.54 (m, 2H), 7.38 (dd, J = 9.6, 2.0 Hz, 1H), 6.41 (q, J = 7.2 Hz, 1H), 3.95 (s, 3H), 2.18 (d, J = 7.2 Hz, 3H). Purity: 99.5%, RT 17.48, ee: 99%. HPLC analysis conditions: Gilson system, Column: Chiralpak Ia 4.6 mm I.D. × 25 cm L; Mobile phase: EtOH/DEA = 100/0.1; Flow rate: 0.5 mL/min; Detector: 254 nm.

Preparation of (*S*)-2-(4-(1-(1-(pyrazolo[1,5-*a*]pyridin-5-yl)-ethyl)-1*H*-[1,2,3]triazolo[4,5-*b*]pyrazin-6-yl)-1*H*-pyrazol-1-yl)-ethanol (30) and (*R*)-2-(4-(1-(1-(pyrazolo[1,5-*a*]pyridin-5-yl)-

ethyl)-1*H*-[1,2,3]triazolo[4,5-*b*]pyrazin-6-yl)-1*H*-pyrazol-1-yl)-ethanol (31). The racemic compound **44** (prepared by a procedure similar to that described for the synthesis of compound **2** using the corresponding 1-(pyrazolo[1,5-*a*]pyridin-5-yl)ethanamine instead of quinolin-6-ylmethanamine) (5 mg) was resolved by chiral HPLC to produce optically pure enantiomers **30** (1.0 mg) and **31** (1.9 mg). HPLC resolution conditions: Gilson system, Column: Dicel IA 20 × 250 mm; Mobile phase: *n*-Hexane/*i*-PrOH/DEA = 6/4/0.1; Flow rate: 8 mL/min; Detector: 254 nm). Compound **44**: Purity: 95.8%, RT 9.28. MS (*m*/*z*): 376 $(M + 1)^+$. ^{1}H NMR (400 MHz, CD_3OD) δ 9.07 (s, 1H), 8.49−8.47 (m, 2H), 8.26 (s, 1H), 7.93 (d, *J* = 2.4 Hz, 1H), 7.78 (s, 1H), 7.01 (dd, *J* = 7.2, 2.0 Hz, 1H), 6.62 (d, *J* = 2.4 Hz, 1H), 6.47 (q, *J* = 6.8 Hz, 1H), 4.33 (t, *J* = 4.2 Hz, 2H), 3.95 (t, *J* = 4.2 Hz, 2H), 2.25 (d, *J* = 6.8 Hz, 3H). Compound **30:** MS (*m*/*z*): 376 $(M + 1)^+$. ^{1}H NMR (400 MHz, CD_3OD) δ 9.08 (s, 1H), 8.50 (s,1 H), 8.50 (d, *J* = 7.2 Hz, 1H), 8.27 (s, 1H), 7.94 (d, *J* = 2.4 Hz, 1H), 7.79 (s, 1H), 7.01(dd, *J* = 7.2, 2.0 Hz, 1H), 6.62 (d, *J* = 1.6 Hz, 1H), 6.48 (q, *J* = 6.8 Hz, 1H), 4.33 (t, *J* = 4.2 Hz, 2H), 3.95(t, *J* = 4.2 Hz, 2H), 2.26 (d, *J* = 6.8 Hz, 3H). Purity: 98.1%, RT 18.44, ee: 96%. Compound **31:** MS (*m*/*z*): 376 $(M + 1)^+$. ^{1}H NMR (400 MHz, CD_3OD) δ 9.08 (s, 1H), 8.51 (s, 1H), 8.49 (d, *J* = 7.6 Hz, 1H), 8.27 (s, 1H), 7.94 (d, *J* = 2.4 Hz, 1H), 7.79 (s, 1H), 7.01 (dd, *J* = 7.2, 2.0 Hz,1H), 6.62 (d, *J* = 2.0 Hz, 1H), 6.48 (q, *J* = 6.8 Hz, 1H), 4.33 (t, *J* = 4.2 Hz, 2H), 3.95 (t, *J* = 4.2 Hz, 2H), 2.26 (d, *J* = 6.8 Hz, 3H). Purity: 90.7%, RT 24.22, ee: 81%. HPLC analysis conditions: Gilson system, Column: Chiralpak Ia 4.6 mm I.D. × 25 cm L; Mobile phase: *n*-Hexane/*i*-PrOH/DEA = 6/4/0.1; Flow rate: 1 mL/min; Detector: 254 nm.

In Vitro Enzymatic Assay. Inhibition of test compound on c-Met kinase activity was measured by using of Transcreener FP ADP Assay (Bellbrook Lab) that was developed to detect ADP generated in the enzyme reaction. The kinase reaction buffer was composed of 67 mM of HEPES/pH = 7.4, 0.013% of Triton X-100, 27 mM of $MgCl_2$, 0.67 mM of $MnCl_2$, 1.25 mM of DTT. Test compound was tested in a 8-point series dilution. The enzymatic reaction contains 0.2 μg/mL of recombinant c-Met catalytic domain (Invitrogen Co.), 25 μg/mL of Poly E4Y substrate (Sigma-Aldrich), 5 μL of tested compound diluted in 20% DMSO, and 10 μM of ATP. All components were diluted in assay buffer. The final concentration of DMSO in the reaction was 4%. ATP was the last component to be added, for initiating the reaction. The reaction mixture was incubated at 25 °C for 45 min. Then ADP detection mixture was added and incubated at 25 °C for additional 1 h. Florescence polarization is measured on TECAN F500 at excitation of 610 nm and emission of 670 nm. Produced ADP concentration was calculated using standard curve obtained in the same study based on the recommendation of manufacturer.

Cell-Based Activity Assay. IC_{50} of test compounds on c-Met autophosphorylation was determined in NCI-H441 cells (American Type Culture Collection, ATCC, Rockville, MD) using human phospho-HGF R/c-MET ELISA kit (R&D System China Co., Ltd.). The assay was carried out according the manufacturer's instruction. Briefly, NCI-H441 cells were plated at a density of 15,000 cells/well in RPMI-1640 medium with 10% FBS in 96-well plates. After incubation overnight, cells were then treated with serially diluted test compounds at 37 °C for 1 h. Then the medium was removed, and cells were lysed in 100 μL/well lysis buffer (1% NP-40, 20 mM Tris/pH = 8.0, 137 mM NaCl, 10% glycerol, 2 mM EDTA, 1 mM activated sodium orthovanadate, 10 mg/mL Aprotinin, 10 mg/mL Leupeptin). The plates containing cell lysate were kept at −80 °C overnight. The next day, the plates were thawed on ice, mixed gently. Twenty-five μL/well of lysates were added into the assay plates precoated with anti-p-Met antibody to detect p-c-Met signal. p-c-Met level was determined at 450 and 570 nm using Labsystems Multiskan K3. The inhibition rate was calculated according to the following equation, and IC_{50} was determined using XLFit2.0 software.

$$\text{Inhibition}(\%) = 100 - 100 \times \{[OD_{450} - OD_{570}]_{\text{compd}} - [OD_{450} - OD_{570}]_{\text{lysis buffer}}\}/\{[OD_{450} - OD_{570}]_{\text{cell}} - [OD_{450} - OD_{570}]_{\text{lysis buffer}}\}$$

where $[OD_{450} - OD_{570}]_{\text{compd}}$ represents the optical density of wells with compound treatment; $[OD_{450} - OD_{570}]_{\text{cell}}$ represents the optical density of wells without compounds treatment; and $[OD_{450} - OD]_{\text{lysis buffer}}$ represents the optical density of wells containing lysis buffer, but without cells.

HGF-Induced Proliferation Assay. NCI-H441 cells were seeded in 96-well plates at 8000 cells/well in RPMI 1640 medium containing 10% FBS. After incubation overnight, cells were starved in FBS-free medium (containing 0.5% BSA) for 16−20 h, then treated with test compounds at different concentrations for 2 h at 37 °C. Recombinant human HGF (R&D System China Co., Ltd.) was added to the working concentration of 50 ng/mL and incubated for additional 72 h at 37 °C in incubator. Ten μL/well of 5 mg/mL of MTT solution was added, and the plates were incubated at 37 °C for additional 4 h. Cell survival was read at 492 nm on Labsystems Multiskan K3. Inhibition rate of compound at each test point was calculated according to following equation and IC_{50} was calculated using XLFit2.0 software.

$$\text{Inhibition}(\%) = 100 - 100 \times \{[OD_{492}]_{\text{compd}} - [OD_{492}]_{\text{cell}}\}/\{[OD_{492}]_{\text{HGF}} - [OD_{492}]_{\text{cell}}\}$$

where $[OD_{492}]_{\text{compd}}$ represents the optical density of cells treated with test compound in the presence of HGF; $[OD_{492}]_{\text{cell}}$ represents the optical density of cells without test compound and HGF; and $[OD_{492}]_{\text{HGF}}$ represents the optical density of cells stimulated with HGF, but without test compound.

In Vivo Inhibition on c-Met Phosphorylation in NCI-H441. *Cell Lines.* NCI-H441, a human nonsmall cell lung adenocarcinoma epithelial cell line with high level of c-Met expression, was grown in RPMI1640 medium containing 10% FBS. MRC-5, a human lung fibroblast cell line with a capability to secrete bioactive human HGF, was cultured in EMEM with 10% FBS. Female athymic mice (6−8 weeks old) were used for study.

Animals. Female athymic mice (6−8 weeks old) were purchased from Shanghai SLAC laboratory animal CO. Ltd. The animals were housed in SPF environment, 4 animals/cage under standard conditions (12:12 h light/dark, 40−70% relative humidity at 20−25 °C), and given free access to Co^{60} radiated-sterile diet and sterile water. The nude mice were quarantined for at least 3 days before implantation.

Establishment of Subcutaneous Xenograft Model. The tumor cells were incubated at 37 °C in a 5% CO_2 incubator until reaching approximately 80% confluence. Cells were detached by 0.05% Trypsin-EDTA, centrifuged at 800 rpm, and the cells were suspended in serum free-medium, and the concentration was adjusted for tumor implantation in nude mice. NCI-H441 2×10^6 and MRC-5 1×10^6 cells were subcutaneously co-implated to the right lateral flank of nude mice.

c-Met Phosphorylation ELISA Assay. Two weeks after cells implantation, when average tumor volume reached 300 mm^3, the animals were randomized and divided into vehicle and compound treated groups. At 6 h after single oral dosing with 3 mg/kg, animals were euthanized, and tumor tissues were harvested and placed into lysis buffer (Cell Signaling Technologies, CAT #9803) containing phosphatase and protease inhibitors (Thermo Scientific, Cat: 1861282). Tumors were homogenized at 28000 rpm for 8 s (Homogenizers, FA25, Fluko), lysate was spun down at 12000 rpm for 15 min twice, and the supernatant was transferred to eppendorf tubes and stored at −80 °C prior to ELISA assay. Protein concentrations were determined by Bio-Rad Protein Assay (Bio-Rad Cat# 500-0006). Total-Met (R&D Systems, DYC358) and phospho-Met ELISA assays (R&D Systems, DYC2480) were performed according to the manufacturer's instructions.

dx.doi.org/10.1021/jm500510f | *J. Med. Chem.* 2014, 57, 7577−7589

In Vivo Efficacy Study in U87MG Xenograft Model. *Test article.* Compound **28** was formulated in 0.5% CMC-Na (pH = 2.1) and stored at 4 °C. Cell line: U87MG, a human glioma cell line with high expression of c-Met, was incubated in EMEM medium with FBS and sodium pyruvate.

Animals. Female athymic mice (6−8 weeks old) were purchased from Shanghai SLAC laboratory animal CO. Ltd. The animals were housed in SPF environment, 4 animals/cage under standard conditions (12:12 h light/dark, 40−70% relative humidity at 20−25 °C) and given free access to Co^{60} radiated-sterile diet and sterile water. The nude mice were quarantined for at least 3 days before implantation. All studies were done in accordance with Hutchison Medipharma Limited Institutional Animal Care and Use Committee (HMPLACUC) guidelines.

Establishment of subcutaneous xenograft model and in vivo efficacy. U87MG tumor cells were inoculated into the flanks of athymic nude mice (3×10^6cells/mouse). When tumor volume reached 200 mm^3, the mice were randomized into vehicle treated and compound **28** treated groups. The animals were orally administered with compound **28** once a day at 1.0, 2.5, and 10.0 mg/kg or treated with vehicle 0.5% CMC-Na at pH = 2.1. Tumor size was measured 2−3 times per week. Tumor volumes were calculated using the formula: TV = (Length × $Width^2$)/2. The percentage of tumor growth inhibition (%TGI = $[1 - (V_t - V_0)_{\text{drug treated}}/(V_t - V_0)_{\text{vehicle control}}] \times 100\%$) was used for evaluation of the antitumor efficacy. V_0 represents mean tumor volume at the first day of treatment; and V_t represents mean tumor volume at the last day of treatment. Animal body weight and behavior were observed during the experiment. Statistical analysis for tumor volume was performed by the student *t* test for a mean comparison.

In vivo PK study. Twelve male mice were randomly divided into two groups (6 mice per group). One group was given an intravenous dose of 2.5 mg/kg dissolved in saline containing 10% Solutol HS 15, 10% ethanol, and 0.25% DMSO. The other group was given an oral dose of 10 mg/kg as a suspension in acidic 0.5% CMC-Na (acidified by HCl to pH = 2.1 before adding compound). In each group, 3 mice were blood-sampled at predose (0), 0.25, 1, 2, 6, and 24 h postdose, while the remaining at 5 min, 0.5, 1.5, 4, and 8 h postdose. At the due time, 100 μL of blood was collected. After centrifugation to get the plasma, the concentration was determined by a LC/MS/MS method.

Mouse Liver Microsome (MLM) Stability Screening Study. The incubations were conducted in duplicate. In general, incubation mixtures consisted of mouse liver microsomes (0.5 mg/mL), test compound (1 μM), $MgCl_2$ (final 3 mM), EDTA (final 1 mM), and NADPH regenerating system (containing 5 mM G-6-P, 1U/mL G-6-PD, and 1 mM NADP, which was prepared in 50 mM potassium phosphate buffer at pH 7.4 and preincubated at 37 °C water-bath for 10 min and then cooled on ice until added into the reaction system) with a final volume of 125 μL. The stock solution of test compound was prepared with DMSO first and then diluted to designated concentration. The contents of organic solvents in the final incubation system were no more than 1% (for DMSO, the controlled margin was 0.1%). The incubation was commenced by putting the incubation system into 37 °C water bath open to the air and maintained for 0 and 30 min. The incubation was typically terminated by adding 125 μL cold acetonitrile containing internal standard. The terminated incubation mixtures were centrifuged at 3000 g for 10 min, and then 10 mL of supernatant was injected for analysis.

Incubation with Liver S9 Fractions. Compound **28** was mixed with human liver S9 fractions (1 mg/mL) in 50 mM phosphate potassium buffer (pH 7.4) containing 3 mM $MgCl_2$ and 1 mM EDTA first on ice-bath. The incubation was conducted with or without NADPH regenerating system to differentiate the contribution of NADPH-dependent enzymes (such as CYP450s and FMO) and NADPH-independent enzymes (enzymes existing in cytosols such as aldehyde oxidase and xanthine oxidase). NADPH regenerating system containing 1 mM NADP, 5 mM glucose-6-phosphate, 1 U/mL glucose-6-phosphate dehydrogenase was preincubated for 10 min prior to adding into the incubation system and then cooled on ice-bath prior to adding into incubation system. The reaction was commenced by putting the incubation system into 37 °C water bath open to the air and maintained for 0 and 60 min and stopped with the addition of an equal volume of ice-cold acetonitrile. Blank samples were also prepared simultaneously with same contents except of using blank reagents to instead compound **28** and incubated for 60 min. All terminated incubation samples were centrifuged at 3000 rpm for 10 min at 4 °C, and then 2400 μL supernatant was aspirated, transferred to other clean tubes, and dried with a nitrogen flow at room temperature. The residues were then reconstituted with 200 μL 50% methanol and injected for LC-MS^n/PDA analysis.

Solubility Test. pH 1.2 buffer: Dissolve 3.73g of potassium chloride in 250 mL of purified water. Add 425 mL of 0.2 M hydrochloric acid. Mix thoroughly, dilute with water to 1000 mL, and adjust the pH of the buffer to 1.2 ± 0.05. pH 7.4 buffer: Dissolve 6.81 g of monobasic sodium phosphate in 250 mL of purified water. Add 195.5 mL of 0.2 M sodium hydroxide solution. Mix thoroughly, dilute with water to 1000 mL, and adjust the pH of the buffer to 7.4 ± 0.05. Accurately weigh 7.9 mg of **28-AO** into a 50 mL volumetric flask, add about 40 mL of mobile phase to dissolve, and dilute to volume with mobile phase, or weigh 10.66 mg of **28** into a 50 mL volumetric flask, add about 40 mL of mobile phase to dissolve, and dilute to volume with mobile phase. Place excess **28-AO** in a 10 mL tube containing 5 mL of buffer solution, or **28** in a 5 mL tube containing 2 mL of buffer solution and shake (3 cm/200time s/min) for 48 h at 20 °C. Then centrifuge for 10 min at 4000 rpm, transfer 1 mL of supernatant into a clean glass container, dilute with mobile phase to a suitable concentration, and measure by a HPLC method.

■ ASSOCIATED CONTENT

Supporting Information

Kinase selectivity data of compound **28**, body weight of compound **28** on U87MG xenograft model in mice, and additional synthetic procedures of the intermediates 1−16 for compounds **9-27B** and **43-44**. This material is available free of charge via the Internet at http://pubs.acs.org.

■ AUTHOR INFORMATION

Corresponding Author

*E-mail: weiguos@hmplglobal.com. Phone: (+86)-21-20673002.

Author Contributions

†These authors contributed equally.

Notes

The authors declare no competing financial interest.

■ ABBREVIATIONS USED

AcOH, acetic acid; AO, aldehyde oxidase; Axl, AXL receptor tyrosine kinase; c-Met, mesenchymal−epithelial transition factor; CMC, carboxymethyl cellulose; DIEA, *N*,*N*-diisopropylethylamine; EtOAc, ethyl acetate; HGF, hepatocyte growth factor; ng, nanogram; Ron, Recepteur d'Origine Nantais Kinase; RTK, receptor tyrosine kinases

■ REFERENCES

(1) Bottaro, D. P.; Rubin, J. S.; Faletto, D. L.; Chan, A. M. L.; Kmiecik, T. E.; Vande Woude, G. F.; Aaronson, S. A. Identification of the hepatocyte growth factor receptor as the c-met proto-oncogene product. *Science* **1991**, *251*, 802−804.

(2) Naldini, L.; Vigna, E.; Narsimhan, R. P.; Gaudino, G.; Zarnegar, R.; Michalopoulos, G. K.; Comoglio, P. M. Hepatocyte growth factor (HGF) timulates the tyrosine kinase activity of the receptor encoded by the proto-oncogene c-MET. *Oncogene* **1991**, *6*, 501−504.

(3) Di Renzo, M. F.; Narsimhan, R. P.; Olivero, M.; Bretti, S.; Giordano, S.; Medico, E.; Gaglia, P.; Zara, P.; Comoglio, P. M. Expression of the Met/HGF receptor in normal and neoplastic human tissues. *Oncogene* **1991**, *6*, 1997−2003.

(4) Kiehne, K.; Herzig, K. H.; Folsch, U. R. c-Met expression in pancreatic cancer and effects of hepatocyte growth factor on pancreatic cancer cell growth. *Pancreas* **1997**, *15*, 35−40.
(5) Shinomiya, N.; Vande Woude, G. F. Suppression of met expression: A possible cancer treatment. *Clin. Cancer Res.* **2003**, *9*, 5085−5090.
(6) Sierra, J. R.; Tsao, M. S. c-Met as a potential therapeutic target and biomarker in cancer. *Ther. Adv. Med. Oncol.* **2011**, *3* (S1), S21−S35.
(7) Qian, F.; Engst, S.; Yamaguchi, K.; Yu, P. W.; Won, K. A.; Mock, L.; Lou, T.; Tan, J.; Li, C.; Tam, D.; Lougheed, J.; Michael Yakes, F.; Bentzien, F.; Xu, W.; Zaks, T.; Wooster, R.; Greschock, J.; Joly, A. H. Inhibition of tumor cell growth, invasion, and metastasis by EXEL-2880 (XL880, GSK1363089), a novel inhibitor of HGF and VEGF receptor tyrosine kinases. *Cancer Res.* **2009**, *69*, 8009−8016.
(8) Schroeder, G. M.; An, Y. M.; Cai, Z. W.; Chen, X. T.; Clark, C.; Cornelius, L. A. M.; Dai, J.; Gullo-Brown, J.; Gupta, A.; Henley, B.; Hunt, J. T.; Jeyaseelan, R.; Kamath, A.; Kim, K.; Lippy, J.; Lombardo, L. J.; Manne, V.; Oppenheimer, S.; Sack, J. S.; Schmidt, R. J.; Shen, G. X.; Stefanski, K.; Tokarski, J. S.; Trainor, G. L.; Wautlet, B. S.; Wei, D.; Williams, D. K.; Zhang, Y. R.; Zhang, Y. P.; Fargnoli, J.; Borzilleri, R. M. Discovery of *N*-(4-(2-amino-3-chloropyridin-4-yloxy)-3-fluorophenyl)-4-ethoxy-1-(4-fluorophenyl)-2-oxo-1,2-dihydropyridine-3-carboxamide (BMS-777607), a selective and orally efficacious inhibitor of the Met kinase superfamily. *J. Med. Chem.* **2009**, *52*, 1251−1254.
(9) Cui, J. J.; McTigue, M.; Nambu, M.; Tran-Dubé, M.; Pairish, M.; Shen, H.; Jia, L.; Cheng, H. M.; Hoffman, J.; Le, P.; Jalaie, M.; Goetz, G. H.; Ryan, K.; Grodsky, N.; Deng, Y. L.; Parker, M.; Timofeevski, S.; Murray, B. W.; Yamazaki, S.; Aguirre, S.; Li, Q. H.; Zou, H.; Christensen, J. Discovery of a novel class of exquisitely selective mesenchymal−epithelial transition factor (c-MET) protein kinase inhibitors and identification of the clinical candidate 2-(4-(1-(quinolin-6-ylmethyl)-1*H*-[1,2,3]triazolo[4,5-*b*]pyrazin-6-yl)-1*H*-pyrazol-1-yl)-ethanol (PF-04217903) for the treatment of cancer. *J. Med. Chem.* **2012**, *55*, 8091−8109.
(10) Underiner, T. L.; Herbertz, T.; Miknyoczki, S. J. Discovery of small molecule c-Met inhibitors: Evolution and profiles of clinical candidates. *Anti-cancer Agents in Med. Chem.* **2010**, *10*, 7−27.
(11) A safety and dose-finding study of JNJ-38877605 in patients with Advance or refractory solid tumor. This study has been terminated. *ClinicalTrials*; National Institutes of Health: Bethesda, MD; http://clinicaltrials.gov/ct2/show/NCT00651365?term=JNJ-38877605&rank=1 (accessed December 4, 2013).
(12) Buchanan, S. G.; Hendle, J.; Lee, P. S.; Smith, C. R.; Bounaud, P. Y.; Jessen, K. A.; Tang, C. M.; Huser, N. H.; Felce, J. D.; Froning, K. J.; Peterman, M. C.; Aubol, B. E.; Gessert, S. F.; Michael Sauder, J.; Schwinn, K. D.; Russell, M.; Rooney, I. A.; Adams, J.; Leon, B. C.; Do, T. H.; Blaney, J. M.; Sprengeler, P. A.; Thompson, D. A.; Smyth, L.; Pelletier, L. A.; Atwell, S.; Holme, K.; Wasserman, S. R.; Emtage, S.; Burley, S. K.; Reich, S. H. SGX523 is an exquisitely selective, ATP-competitive inhibitor of the MET receptor tyrosine kinase with antitumor activity in vivo. *Mol. Cancer Ther.* **2009**, *8*, 3181−3190.
(13) Diamond, S.; Boer, J.; Maduskuie, T. P., Jr.; Falahatpisheh, N.; Li, Y.; Yeleswaram, S. Species-specific metabolism of SGX523 by aldehyde oxidase and the toxicological implications. *Drug Metab. Dispos.* **2010**, *38* (8), 1277−1285.
(14) Albrecht, B. K.; Harmange, J. C.; Bauer, D.; Berry, L.; Bode, C.; Boezio, A. A.; Chen, A.; Choquette, D.; Dussault, I.; Fridrich, C.; Hirai, S.; Hoffman, D.; Larrow, J. F.; Kaplan-Lefko, P.; Lin, J.; Lohman, J.; Long, A. M.; Moriguchi, J.; O'Connor, A.; Potashman, M. H.; Reese, M.; Rex, K.; Siegmund, A.; Shah, K.; Shimanovich, R.; Springer, S. K.; Teffera, Y.; Yang, Y. J.; Zhang, Y. H.; Bellon, S. F. Discovery and optimization of triazolopyridazines as potent and selective inhibitors of the c-Met kinase. *J. Med. Chem.* **2008**, *51*, 2879−2882.
(15) Cui, J. J.; Shen, H.; Tran-Dube, M.; Nambu, M.; McTigue, M.; Grodsky, N.; Ryan, K.; Yamazaki, S.; Aguirre, S.; Parker, M.; Li, Q. H.; Zou, H.; Christensen, J. Lessons from (*S*)-6-(1-(6-(1-Methyl-1*H*-pyrazol-4-yl)-[1,2,4]triazolo[4,3-*b*]pyridazin-3-yl)ethyl)quinoline (PF-04254644), an inhibitor of receptor tyrosine kinase c-Met with high protein kinase selectivity but broad phosphodiesterase family inhibition leading to myocardial degeneration in rats. *J. Med. Chem.* **2013**, *56*, 6651−6665.
(16) Ye, L. B.; Tian, Y. X.; Li, Z. H.; Jin, H.; Zhu, Z. G.; Wan, S. H.; Zhang, J. Y.; Yu, P. J.; Zhang, J. J.; Wu, S. G. Design, synthesis and molecular docking studies of some novel spiro[indoline-3,4′-piperidine]-2-ones as potential c-Met inhibitors. *Eur. J. Med. Chem.* **2012**, *50*, 370−375.
(17) Norman, M. H.; Andrews, K. L.; Bo, Y. Y.; Booker, S. K.; Caenepeel, S.; Cee, V. J.; D'Angelo, N. D.; Freeman, D. J.; Herberich, B. J.; Hong, F.; Jackson, C. L. M.; Jiang, J.; Lanman, B. A.; Liu, L. B.; McCarter, J. D.; Mullady, E. L.; Nishimura, N.; Pettus, L. H.; Reed, A. B.; Miguel, T. S.; Smith, A. L.; Stec, M. M.; Tadesse, S.; Tasker, A.; Aidasani, D.; Zhu, X. C.; Subramanian, R.; Tamayo, N. A.; Wang, L.; Whittington, D. A.; Wu, B.; Wu, T.; Wurz, R. P.; Yang, K.; Zalameda, L.; Zhang, N.; Hughes, P. E. Selective class I phosphoinositide 3-kinase inhibitiors: optimization of a series of pyridyltriazines leading to the identification of a clinical candidate, AMG 511. *J. Med. Chem.* **2012**, *55*, 7796−7816.
(18) The manuscript about detailed metabolic study of compound **28** is in preparation.
(19) (a) Phase I study of Volitinib (hmpl-504) in patients with advanced solid tumors. . and A food effect phase I study of Volitinib in healthy subjects. This study is recruiting participants. *ClinicalTrials*; National Institutes of Health: Bethesda, MD; http://www.clinicaltrials.gov/ct2/results?term=volitinib&Search=Search (accessed December 4, 2013). (b) A phase II trial to evaluate the efficacy of AZD6094 (hmpl-504) in patients with papillary renal cell carcinoma (PRCC). This study is recruiting participants. *ClinicalTrials*; National Institutes of Health: Bethesda, MD; http://www.clinicaltrials.gov/ct2/show/NCT02127710?term=AZD6094&rank=1 (accessed April 23, 2014).
(20) Gavine, P. R.; Fan, S. M.; Fu, H. H.; Han, L.; Liu, Y. J.; Lv, J.; Qing, W. G.; Ren, Y. X.; Su, W. G.; Su, X. Y.; Wang, H. Y.; Xie, L.; Xu, S. L.; Xu, W.; Yin, X. L.; Yu, Y. J.; Zhang, T. W.; Wang, Q. M. Volitinib (HMPL504), a novel, selective and potent cMET inhibitor, is efficacious in primary tumor models of cMET-driven gastric cancer. *Cancer Res.* **2013**, *73*(8), Supplement 1, doi:10.1158/1538-7445. AM2013−928 Proceedings: AACR 104th Annual Meeting 2013; Washington, DC, Apr 6−10, 2013;. Abstr, 928.
(21) Gu, Y.; Sai, Y.; Wang, J.; Xia, S. M.; Wang, G. L.; Zhao, Y. S.; Zhang, L.; Yang, W. Q.; Dai, G. X.; Zhang, W. H.; Gong, Q. S.; Tian, Z. P.; Su, W. G. Preclinical disposition and pharmacokinetics of volitinib, a novel selective cMet inhibitor. *Cancer Res.* **2013**, *73*(8), Supplement 1, doi:10.1158/1538-7445. AM2013−3371 Proceedings: AACR 104th Annual Meeting 2013, Washington, DC, Apr 6−10, 2013; Abstr, 3371.
(22) Zhou, F.; Ren, Y. X.; Cui, Y. M.; Chen, H. Y.; Jiao, L. X.; Dai, G. X.; Fan, S. M.; Sun, J. N.; Yu, Y. J.; Sai, Y.; Gu, Y.; Qing, W. G.; Su, W. G. Synergistic effect of c-Met inhibitor volitinib in combination with EGFR inhibitor Gefitnib on EGFR-TKI resistant NSCLC model HCC827C4R harboring acquired Met gene amplification. *Cancer Res.* **2013**, *73*(8), Supplement 1, doi:10.1158/1538-7445. AM2013−971 Proceedings: AACR 104th Annual Meeting 2013, Washington, DC, Apr 6−10, 2013; Abstr, 971.
(23) D'Cruz, C.; Frigault, M.; Adam, A.; Shen, M. H.; Beran, G.; Barry, E.; Gavine, P.; Ren, Y. X.; Fan, S. M.; Zhou, F.; Qing, W. G.; Zinda, M.; Su, W. G.; Clark. E. Targeting MET in preclinical models to support the clinical development of Volitinib in NSCLC. Presented at American Association for Cancer Research (AACR) 105th Annual Meeting , San Diego, CA, Apr 5−9, 2014; AACR: Philadelphia, PA, 2014; Abstr, 3114.
(24) Su, W. G.; Dai, G. X.; Jia, H.; Qing, W. G.; Ren, Y. X.; Cui, Y. M.; Zhou, F.; Jiao, L. X.; Gu, Y.; Wang, J.; Ren, H. C.; Sai, Y.; Li, N.; Yan, J.; Wang, M.; Mu, H.; Qi, C.; D'Cruz, C.; Gavine, P.; Frigault, M.; Clark, E. Discovery, preclinical and early clinical evaluation of volitinib: A potent and selective c-Met kinase inhibitor. Presented at American Association for Cancer Research (AACR) 105th Annual Meeting , San Diego, CA, Apr 5−9, 2014; AACR: Philadelphia, PA, 2014.

(25) Cheng, H. M.; Cui, J. J.; Hoffman, E. J.; Jia, L.; Kania, S. R.; Le, P. T. Q.; Nambu, D. M.; Pairish, A. M.; Shen, H.; Tran-dube, B. M. Triazolopyridazine derivatives. PCT International Patent Application WO2007138472, February 7, 2007.